

# Journal Pre-proof

Synthesis and characterization of soluble donor-acceptor type copolymers based on benzotriazole, quinoxaline and benzene units with multicolor electrochromism

Yan Zhang, Hongmei Du, Yiming Yin, Yunyun Dong, Jinsheng Zhao, Zhen Xu



PII: S1566-1199(19)30541-5

DOI: <https://doi.org/10.1016/j.orgel.2019.105514>

Reference: ORGELE 105514

To appear in: *Organic Electronics*

Received Date: 4 September 2019

Revised Date: 16 October 2019

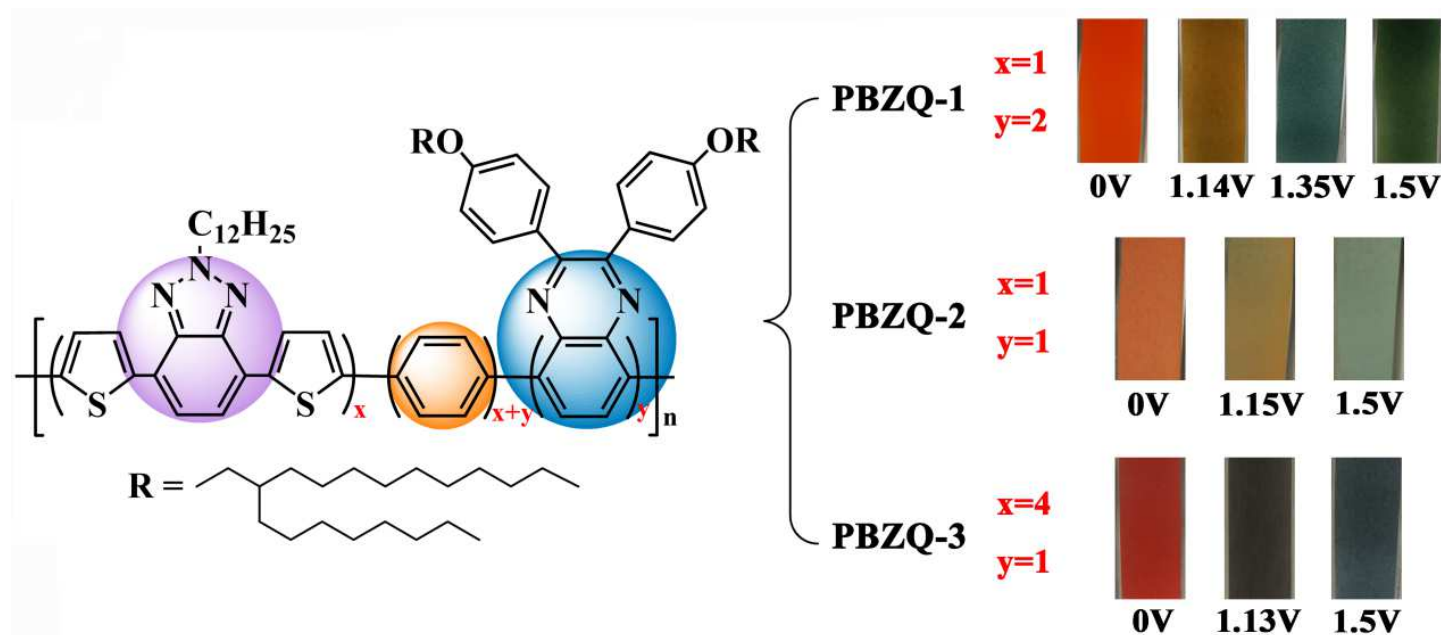
Accepted Date: 17 October 2019

Please cite this article as: Y. Zhang, H. Du, Y. Yin, Y. Dong, J. Zhao, Z. Xu, Synthesis and characterization of soluble donor-acceptor type copolymers based on benzotriazole, quinoxaline and benzene units with multicolor electrochromism, *Organic Electronics* (2019), doi: <https://doi.org/10.1016/j.orgel.2019.105514>.

This is a PDF file of an article that has undergone enhancements after acceptance, such as the addition of a cover page and metadata, and formatting for readability, but it is not yet the definitive version of record. This version will undergo additional copyediting, typesetting and review before it is published in its final form, but we are providing this version to give early visibility of the article. Please note that, during the production process, errors may be discovered which could affect the content, and all legal disclaimers that apply to the journal pertain.

© 2019 Published by Elsevier B.V.

## Graphical Abstract



# Synthesis and characterization of soluble donor-acceptor type copolymers based on benzotriazole, quinoxaline and benzene units with multicolor electrochromism

Yan Zhang<sup>1</sup>, Hongmei Du<sup>1</sup>, Yiming Yin<sup>2</sup>, Yunnyun Dong<sup>2</sup>, Jinsheng Zhao<sup>1,\*</sup>, Zhen Xu<sup>3,\*</sup>

<sup>1</sup>Shandong Provincial Key Laboratory of Chemical Energy Storage and Novel Cell Technology, Liaocheng University, Liaocheng, 252059, P.R. China

<sup>2</sup>College of Chemistry and Chemical Engineering, Liaocheng University, Liaocheng, 252059, P.R. China

<sup>3</sup>School of Chemistry and Chemical Engineering, Shandong University of Technology, Zibo, 255049, P.R. China

\*Correspondence: [j.s.zhao@163.com](mailto:j.s.zhao@163.com) (J.S.Zhao); [xuzhen@sdut.edu.cn](mailto:xuzhen@sdut.edu.cn) (Z. Xu)

## Abstract

Three soluble donor-acceptor (D-A) type copolymers employing benzene (B) as donor, (2-dodecyl-4,7-di(thiophen-2-yl)-2H-benzo[d][1,2,3]triazole (Z) and 2,3-bis((4-(2-octyldodecyl)oxy)phenyl)-quinoxaline (Q) as acceptors were synthesized through chemical polymerization. A variety of characterization methods such as cyclic voltammetry, UV-vis spectroscopy, colorimetry and thermogravimetric analysis were executed to detect the electrochromic properties of polymers. All the polymers displayed multicolor in the redox process with medium band gaps, and different molar ratio of B/Z/Q allowed them to cover diverse color changes, containing orange-red/brown-yellow/cyan/green ((PBZQ-1), orange-red/yellow/light grass green (PBZQ-2), and red/black/grey-blue (PBZQ-3). The multichromism of the polymers involved RGB and black colors. Meanwhile, with the increase of Z unit ratio and the decrease of Q unit ratio, the polymer demonstrated the reduced onset oxidation potential and optical band gap, as well as the different kinetic parameters. Moreover, the three polymers exhibited good solubility, desirable thermal stability, relatively large optical contrast and high coloration efficiency. The above positive

results implied that these copolymers were expected to be the credible candidates for the electrochromic devices with commercial values.

Keywords: D-A type copolymer; multichromism; soluble; benzotriazole; quinoxaline

## 1. Introduction

Conductive polymer (CP) is a class of macromolecular material which has not only the optoelectronic property of metal and inorganic semiconductor, but also the flexible mechanical property and processability of the polymer [1]. Optically responsive CPs that reveal electrochromism have attracted much attention in recent years owing to their advantages of multiple color changes, molecular structure designability, processability, low cost, and so on [2-4]. Although more and more electrochromic polymers have been investigated, multichromic polymers remain a fascinating goal for researchers due to their potential commercial values in smart window and optical display applications [5,6]. Multicolor polymers presenting green or black are rare because green color requires two simultaneous absorptions at red and blue regions and black color needs the complete absorptions in the entire visible region, and therefore it is necessary to design and develop this species [7-9].

Among different methods of color tuning, preparing donor-acceptor (D-A) type polymer is considered as the most popular and powerful strategy as introducing different sorts of donors and acceptors into a same polymer chain can adjust the intra-molecular charge transfer (ICT) effect availably, thereby regulating the polymer optical property [2,10,11]. In general, most D-A type electrochromic polymers tend to show two colors, and only a small number of reported polymers based on triarylamine [12,13], naphthalene bisimide [14], benzotriazole [15], benzothiadiazole [16], quinoxaline [17], etc. exhibit respective impressive multicolor. Moreover, D-A approach is advantageous to reduce the band gap of the polymer and hence optimizes the optical and electronic performances [11]. Another property of concern for the electrochromic polymer is the solubility since the soluble polymer can reduce the fabrication and processing costs by printing, spraying and coating methods. For the D-A type polymer, introducing proper long alkyl side chains in the donors and

acceptors can improve the solubility effectively, and meanwhile, it also can impact the electronic properties including band gap, oxidation potential, and stability [7,18]. Here, we are committed to exploring soluble multichromic polymers through designing double acceptor type D-A structure.

In various D-A type molecules, benzotriazole has always been the research hotspot as an electron-deficient acceptor unit since the benzotriazole-based electrochromic polymer usually combines multiple desired properties in a single polymer such as multichromism, transmissive state, dual type dopability, good solubility and excellent kinetic performance [19,20]. Toppare group synthesized a series of representative benzotriazole bearing polymers [21-23], among which poly((2-dodecyl-4,7-di(thiophen-2-yl)-2H-benzo[d][1,2,3]triazole) (PTBT) was considered to be a significant breakthrough in numerous electrochromic materials due to its multi-color changes including all RGB (red, green, blue) colors, black and transmissive states [21]. Herein, the structure of PTBT was introduced into the new polymer main chains in order to utilize its distinctive properties.

Quinoxaline, as another popular acceptor unit in the D-A type polymer, has been proved to be a desirable building block for a low band gap conjugated polymer which is attributed to its imine nitrogens (C=N) with strong electron withdrawing character [24]. Besides, the quinoxaline structure provides a rigid coplanar backbone which can form a highly extended  $\pi$ -electron system with strong  $\pi$ -stacking in the polymer [25]. Also, it is convenient for quinoxaline unit to introduce other substituents on its 2 and 3 positions, thus enhancing the optoelectronic property and the solubility of the corresponding conjugated polymer [24]. With the help of quinoxaline, many high performance electrochromic polymers were synthesized, and especially some neutral state green polymers with dual type dopability and narrow band gap (less than 1.5 eV) were obtained [26-28].

Our group also synthesized a series of D-A type conductive polymers based on benzotriazole or quinoxaline units which showed different color changes and favorable photoelectric properties [25,29-31]. However, in this work, we attempted to incorporate benzotriazole and quinoxaline together as the double acceptor in a same

D-A type copolymer, and expected the novel copolymers could combine the advantages of the two acceptor units and present desired multichromism, good solubility and processability, as well as low band gap. Though employing benzene (B) as the donor, (2-dodecyl-4,7-di(thiophen-2-yl)-2H-benzo[d][1,2,3]triazole (Z) and 2,3-bis((4-(2-octyldodecyl)oxy)phenyl)-quinoxaline (Q) as the acceptors, a kind of donor-acceptor (1)-donor-acceptor (2) (D-A<sub>1</sub>-D-A<sub>2</sub>) type copolymer were synthesized by Suzuki cross coupling reaction.

The two flanking thiophene groups adjacent to benzotriazole in the Z units, as the  $\pi$ -bridges, played a role of not only improving the planarity of the polymer backbone but also reducing the steric hindrance between Z and other units [32]. In the Q units, the two phenyl groups connected on quinoxaline were aimed to expand the conjugation length and reduce the steric hindrance of the alkoxy long chains [33]. And the alkyl and alkoxy side chains linked on the benzotriazole and quinoxaline molecules were used to increase the solubility of the polymer [18,34]. By changing the molar ratio of different units, three copolymers namely PBZQ-1 (B: Z: Q = 3: 1: 2), PBZQ-2 (B: Z: Q = 2: 1: 1) and PBZQ-3 (B: Z: Q = 5: 4: 1) were prepared, and as predicted, these copolymers exhibited different multicolor in the redox process with good solubility, satisfactory kinetic property and favorable thermal stability. In particular, the color changes of the three polymers covered RGB and black colors, which were very important electrochromic features for their actual utilizations.

## 2. Experimental Section

### 2.1. Materials

4,7-dibromobenzo[c][1,2,5]thiadiazole (98%), and 1,2-bis(4-methoxyphenyl)ethane-1,2-dione (98%) were purchased from Puyang HuiCheng electronic material co., Ltd (Puyang, China). Sodium borohydride (NaBH<sub>4</sub>, 98%), hydrogen bromide (HBr, 40%), bromine (Br<sub>2</sub>, 99.9%), N-bromosuccinimide (NBS, 98.0%), 1-bromo-2-octyldodecane, tetrabutylammonium bromide (TBAB), anhydrous potassium carbonate (K<sub>2</sub>CO<sub>3</sub>), anhydrous sodium carbonate (Na<sub>2</sub>CO<sub>3</sub>) tributyl(thiophen-2-yl)stannane, 1,2,3-benzotriazole (99%), potassium tert-butoxide

(*t*-BuOK, 98%), bromododecane ( $C_{12}H_{25}Br$ , 98%), bis-(triphenylphosphine) dichloropalladium ( $Pd(PPh_3)_2Cl_2$ ,  $\geq 98\%$ ), tetrakis(triphenylphosphine)palladium ( $Pd(PPh_3)_4$ , 99.0%), tetrabutylammonium fluoride ( $N(n-Bu)_4F$ ), 1,4-bis(4,4,5,5-tetramethyl-1,3,2-dioxaborolan-2-yl)benzene ( $>98.0\%$ ) and tetrabutyl-ammonium hexafluorophosphate ( $TBAPF_6$ , 98%) were purchased from Aladdin Chemical Co., Ltd. (Shanghai, China). Ethanol (EtOH, 99.9%), methanol (MeOH, 99.7%), toluene (99.9%), glacial acetic acid (HAc, 99.9%), magnesium sulfate ( $MgSO_4$ ), chloroform, *n*-hexane and *N,N*-dimethylformamide (DMF) were bought from Sinopharm Chemical Reagent Co., Ltd. (Shanghai, China). Dichloromethane (DCM) and acetonitrile (ACN) were bought from Tedia Co., Inc. (Fairfield, Ohio, USA). Indium-tin-oxide (ITO) coated glass (sheet resistance:  $< 10 \Omega/sq$ ) were bought from Shenzhen CSG Display Technologies (Shenzhen, China).

## 2.2. Syntheses of the polymers

### 2.2.1. Synthesis of 5,8-dibromo-2,3-bis(4-((2-octyldodecyl)oxy)phenyl)quinoxaline (3)

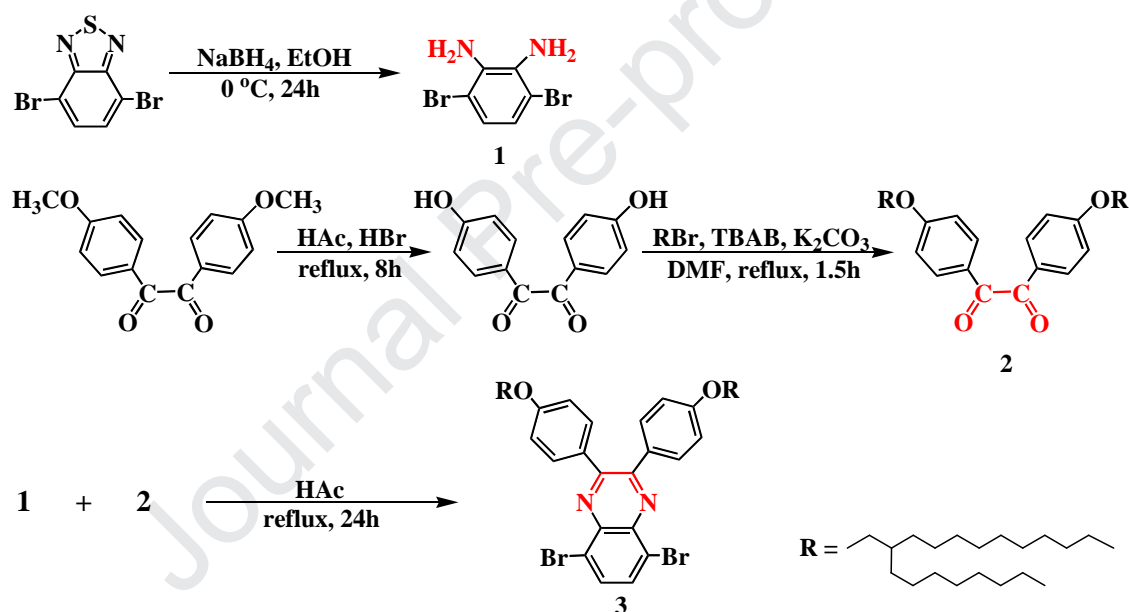
The synthetic route of product 3 was illustrated in Scheme 1. The compounds 3,6-dibromobenzene-1,2-diamine (1) [26] and 1,2-bis(4-((2-octyldodecyl)oxy)phenyl)ethane-1,2-dione (2) [35] were synthesized in accordance with the methods reported in the literatures.

The compound 1 acquired in the end was the white flocculent solids.  $^1H$  NMR (400 MHz,  $CDCl_3$ ):  $\delta$  6.84(s, 2H), 3.89(s, 4H);  $^{13}C$  NMR (100 MHz,  $CDCl_3$ )  $\delta$  133.71, 123.24, 109.68(see supporting information Fig. S1)

The compound 2 acquired in the end was the yellow-green oily liquid.  $^1H$  NMR(400 MHz,  $CDCl_3$ ,  $\delta$  ppm)  $\delta$ =7.93 (d, 4H, ArH), 6.95 (d, 4H, ArH), 3.90 (d, 4H), 1.80 (m, 2H), 1.26(m, 64H), 0.88 (t, 12H).  $^{13}C$  NMR ( $CDCl_3$ , 101 MHz, ppm)  $\delta$  = 193.52, 164.69, 132.29, 126.07, 114.70, 71.32, 37.79, 31.88, 31.25, 29.93, 29.56, 29.29, 26.78, 22.65, 14.06 (see supporting information Fig. S2).

As shown in Scheme 1, 0.665 g compound 1 (2.50 mmol) and 2.0 g compound 2 (2.50 mmol) were dissolved by 100 ml HAc in a round-bottom flask. After that, 20 ml *n*-hexane was added to this mixture to increase the solubility of compound 2 in HAc.

After argon was injected to eliminate residual oxygen, the mixture was heated and refluxed for 24 hours. Then, the solution was extracted with deionized water and n-hexane. After the solvent of organic phase was removed by distillation under reduced pressure, the crude product was obtained and further refined by column chromatography using hexane/DCM (3:1, v/v) as eluent. The pure product 3 was the yellow-green waxy solid.  $^1\text{H}$  NMR(400 MHz,  $\text{CDCl}_3$ ,  $\delta$  ppm)  $\delta$ =7.84 (s, 2H, ArH), 7.66 (d, 4H, ArH), 6.89 (d, 4H, ArH), 3.87 (d, 4H), 1.78 (m, 2H), 1.27 (m, 64H), 0.88 (t, 12H).  $^{13}\text{C}$  NMR ( $\text{CDCl}_3$ , 101 MHz, ppm)  $\delta$  = 160.74, 153.55, 139.00, 132.41, 131.60, 130.30, 123.43, 114.42, 71.07, 37.92, 31.89, 31.36, 30.00, 29.62, 29.31, 26.84, 22.66, 14.08 (see supporting information Fig. S3).



**Scheme 1.** The synthetic route of 5,8-dibromo-2,3-bis(4-((2-octyldodecyl)oxy)phenyl)quinoxaline.

### 2.2.2. Synthesis of 4,7-bis(5-bromothiophen-2-yl)-2-dodecyl-2H-benzo[d][1,2,3]triazole (6)

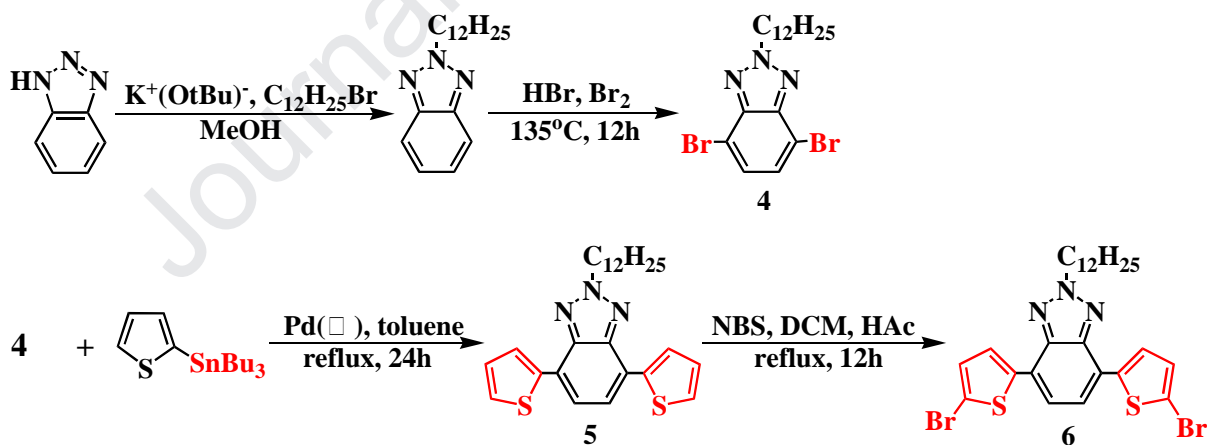
The synthetic route of product 6 was exhibited in Scheme 2. The compound 4,7-dibromo-2-dodecyl-2H-benzo[d][1,2,3]triazole (4) [22,23] was synthesized according to the literatures.

The compound 4 acquired in the end was the yellow-white solid powder.  $^1\text{H}$  NMR(400 MHz,  $\text{CDCl}_3$ ,  $\delta$  ppm)  $\delta$ =7.42 (s, 2H, ArH), 4.76 (t, 2H), 2.13 (m, 2H), 1.24 (m, 18H), 0.86 (t, 3H).  $^{13}\text{C}$  NMR ( $\text{CDCl}_3$ , 101 MHz, ppm)  $\delta$  = 143.68, 129.44, 109.96,



57.43, 31.86, 30.15, 29.55, 29.44, 29.28, 26.93, 26.47, 22.64, 14.07 (see supporting information Fig. S4).

As shown in Scheme 2, firstly, 2.0 g compound 4 (4.5mmol), 4.2 g tributyl(thiophen-2-yl)stannane (11.25 mmol) and 0.2 g  $\text{Pd}(\text{PPh}_3)_2\text{Cl}_2$  (0.285 mmol) were added to 100 ml toluene. After 30 min of argon flow, the mixture was refluxed for 24 h to acquire 2-dodecyl-4,7-di(thiophen-2-yl)-2H-benzo[d][1,2,3]triazole (5). Secondly, weigh accurately 1.2 g compound 5 (2.64 mmol) and 1.1 g NBS (6.2 mmol) to a round-bottomed flask equipped with 35ml HAc and 35ml DCM. Then the solution was heated to reflux for 12 h avoiding light. After completion, the mixture was extracted with DCM and the crude product was purified by silica gel column chromatography. The pure product 6 was the bright yellow solid.  $^1\text{H}$  NMR (400 MHz,  $\text{CDCl}_3$ ,  $\delta$  ppm)  $\delta$ =7.78 (d, 2H, ArH), 7.50 (s, 2H), 7.12(d, 2H), 4.79 (t, 2H), 2.18 (m, 2H), 1.25 (m, 18H), 0.87 (t, 3H).  $^{13}\text{C}$  NMR ( $\text{CDCl}_3$ , 101 MHz, ppm)  $\delta$  = 141.72, 141.22, 130.84, 126.91, 123.00, 122.18, 113.14, 56.92, 31.88, 30.00, 29.59, 29.51, 29.40, 29.30, 28.98, 26.55, 22.65, 14.08 (see supporting information Fig. S5).



**Scheme 2.** The synthetic route of 4,7-bis(5-bromothiophen-2-yl)-2-dodecyl-2H-benzo[d][1,2,3]triazole.

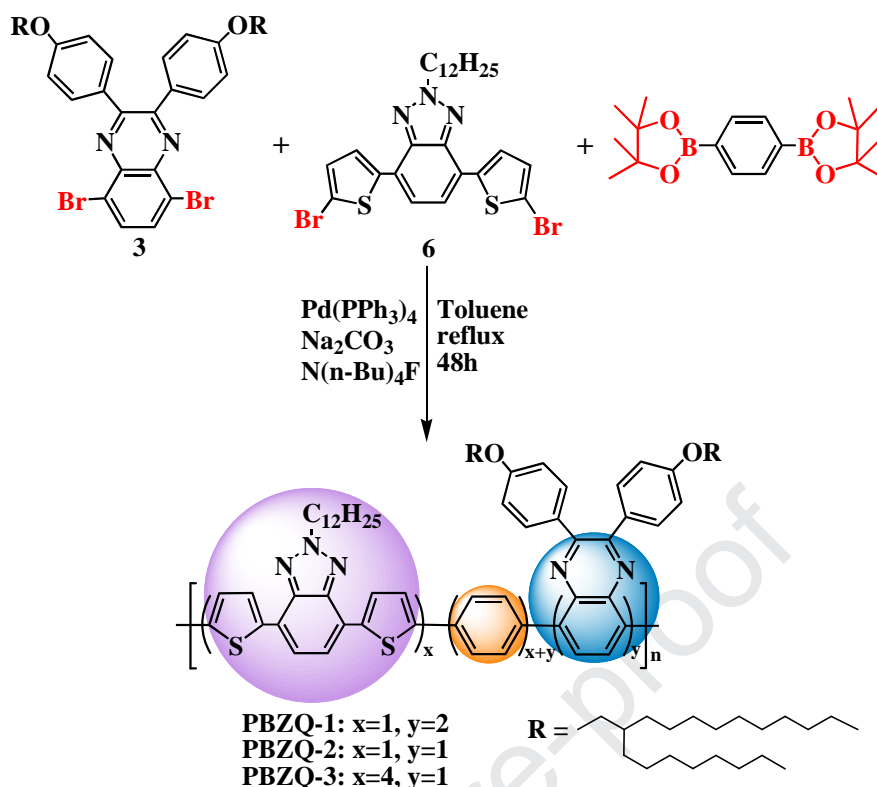
### 2.2.3. Syntheses of PBZQ-1, PBZQ-2 and PBZQ-3

As shown in Scheme 3, Suzuki cross-coupling reaction was used to synthesize the copolymer. 0.2396 g 1,4-Bis(4,4,5,5-tetramethyl-1,3,2-dioxaborolan-2-yl)benzene (0.7259 mmol), 0.5000 g compounds 3 (0.4839 mmol), 0.1475g compounds 6 (0.2420 mmol), 0.042 g  $\text{Pd}(\text{PPh}_3)_4$  (0.0360 mmol), 0.0150 g  $\text{N}(\text{n-Bu})_4\text{F}$  (0.0570 mmol) and 60

ml NaCO<sub>3</sub> aqueous solution (2 mol/L) were added to 90ml toluene, and the mixture was heated to reflux for 48h in the protection of argon. After completion of the reaction, toluene was distilled off under reduced pressure and then the crude product was recrystallized with methanol. The acquired solid powder still needed to be extracted in adipose extractor with methanol and acetone as the solvent in sequence until the solvent was colorless. The resulting PBZQ-1 was bright red solid. <sup>1</sup>H NMR(400 MHz, CDCl<sub>3</sub>,  $\delta$  ppm)  $\delta$ =8.12 (d, 2H), 8.05-7.99 (m, 2H), 7.90 (s, 2H), 7.80-7.34 (m, 8H), 7.21-7.00 (m, 2H), 6.84 (s, 5H), 3.81 (s, 4H), 2.17 (s, 2H), 1.74 (s, 2H), 1.50-0.98 (m, 120H), 0.86 (s, 27H) (see supporting information Fig. S6a). The gel permeation chromatography (GPC) data:  $M_w$  = 24.5 kDa,  $M_n$  = 15.3 kDa, polydispersity index = 1.60.

The synthetic methods of PBZQ-2 and PBZQ-3 were identical with PBZQ-1 except for the different ratio of monomers. For PBZQ-2, the amounts of reagents were 0.3194 g 1,4-bis(4,4,5,5-tetramethyl-1,3,2-dioxaborolan-2-yl)benzene (0.9678 mmol), 0.5000 g compounds 3 (0.4839mmol), 0.2949 g compounds 6 (0.4839 mmol), 0.060 g Pd(PPh<sub>3</sub>)<sub>4</sub> (0.0520 mmol), 0.015g N(n-Bu)4F (0.0570 mmol), 60 ml NaCO<sub>3</sub> (2 mol/L) aqueous solution and 90 ml toluene. The product PBZQ-2 was also bright red solid. <sup>1</sup>H NMR (400 MHz, CDCl<sub>3</sub>,  $\delta$  ppm)  $\delta$ =8.13-7.90 (m, 4H), 7.67-7.38 (m, 6H), 7.12-7.08 (m, 2H), 6.83 (s, 4H), 3.81 (s, 2H), 2.17 (s, 2H), 1.51-0.95 (m, 70H), 0.85 (s, 15H) (see supporting information Fig. S6b). The GPC data:  $M_w$  = 23.9 kDa,  $M_n$  = 15.1 kDa, polydispersity index = 1.58.

For PBZQ-3, the amounts of reagents were 0.3383 g 1,4-bis(4,4,5,5-tetramethyl-1,3,2-dioxaborolan-2-yl)benzene (1.025 mmol), 0.2118 g compounds 3 (0.205 mmol), 0.5000 g compounds 6 (0.8200 mmol), 0.0600 g Pd(PPh<sub>3</sub>)<sub>4</sub> (0.0520 mmol), 0.0150 g N(n-Bu)4F (0.0570 mmol), 60 ml NaCO<sub>3</sub> aqueous solution (2 mol/L) and 90 ml toluene. The product PBZQ-3 was dark red solid. <sup>1</sup>H NMR(400 MHz, CDCl<sub>3</sub>,  $\delta$  ppm)  $\delta$ =7.87-7.72 (d, 2H), 7.70-7.42 (m, 3H), 7.23-6.99 (m, 4H), 6.98-6.65 (d, 5H), 3.87 (s, 4H), 2.77 (s, 3H), 1.95-1.63 (m, 4H), 1.49-1.05 (m, 52H), 0.87 (s, 15H) (see supporting information Fig. S6c). The GPC data:  $M_w$  = 22.9 kDa,  $M_n$  = 15.9 kDa, polydispersity index = 1.44.



**Scheme 3.** The synthetic route of PBZQ-1, PBZQ-2 and PBZQ-3.

### 2.3. Instrument and characterization

The  $^1\text{H}$  NMR and  $^{13}\text{C}$  NMR spectra measurements were carried out on a Varian AMX 400 spectrometer (Varian Inc., Santa Clara, CA, USA) with tetramethylsilane (TMS) as the internal standard. The GPC analysis was performed by a Waters 2414 system (Waters Inc., Milford, MA, USA) with PSS SDV 100000  $\text{A}^0$   $5\ \mu\text{m}$   $8 \times 300\ \text{mm}$  column, and the UV-vis detector. The fourier transform infrared (FT-IR) spectra were recorded on a Nicolet 6700 FTIR spectrometer (Thermo Fisher Scientific Inc., Waltham, MA, USA). The X-ray photoelectron microscopy (XPS) tests were executed by a Thermo Escalab Xi+ (Thermo Fisher Scientific, Waltham, MA, USA) using a monochromated Al X-ray resource at 1486.6 eV.

Before the electrochemical and spectroelectrochemical experiments, the polymer solutions (5 mg/mL) were prepared with chloroform as solvent, and then spray-coated onto the ITO glasses to create the thin films (active area of  $0.9\ \text{cm} \times 3.0\ \text{cm}$ ). The electrochemical experiments were performed in a one-compartment cell under air atmosphere by a CHI 760 C Electrochemical Workstation (Shanghai Chenhua Instrument Co., Shanghai, China), using a ITO glasses as working electrode (WE), a

platinum ring as counter electrode (CE), and a silver wire (0.03 V vs. saturated calomel electrode, SCE) as pseudo-reference electrode (RE).

The UV-Vis-NIR spectra were recorded on a Varian Cary 5000 spectrophotometer (Varian Inc., Santa Clara, CA, USA), and the required applied potentials were controlled synchronously by the aforementioned electrochemistry workstation. The kinetic and colorimetric data were also obtained by the Varian Cary 5000 spectrophotometer. The thicknesses of the polymer films were detected on a KLA-Tencor D-100 step profiler (KLA-Tencor Inc., Milpitas, CA, USA).

All digital photographs showing polymer colors were taken by a Canon Power Shot A3000 IS digital camera (Canon Inc., Tokyo, Japan). The thermogravimetric analysis (TGA) was executed by a Netzsch STA449C TG/DSC simultaneous thermal analyzer (Netzsch Inc., Bavaria, Germany) in nitrogen atmosphere with 15 °C/min heating rate.

### 3. Results and discussion

#### 3.1. FT-IR spectra

FT-IR spectra were measured to further confirm the structures of the copolymers, and the results were shown in Fig.1. The following peaks were identified in the spectrum of PBZQ-1: 2923  $\text{cm}^{-1}$  and 2852  $\text{cm}^{-1}$  (aliphatic C-H stretching vibrations), 1605  $\text{cm}^{-1}$ , 1577  $\text{cm}^{-1}$ , 1509  $\text{cm}^{-1}$  and 1492  $\text{cm}^{-1}$  (skeletal vibrations in benzene, thiophene, benzotriazole and quinoxaline rings), 1465  $\text{cm}^{-1}$ , 1400  $\text{cm}^{-1}$  and 1377  $\text{cm}^{-1}$  (C-H in-plane bending vibrations in methylene and methyl), 1336  $\text{cm}^{-1}$ , 1289  $\text{cm}^{-1}$ , 1172  $\text{cm}^{-1}$  and 1111  $\text{cm}^{-1}$  (C-S, C-N and N-N stretching vibrations in thiophene, benzotriazole and quinoxaline rings), 1247  $\text{cm}^{-1}$  and 1030  $\text{cm}^{-1}$  (C-O-C stretching vibrations), 987  $\text{cm}^{-1}$  (C-H in-plane bending vibrations in benzene, thiophene, benzotriazole and quinoxaline rings), 831  $\text{cm}^{-1}$ , 801  $\text{cm}^{-1}$ , 721  $\text{cm}^{-1}$  (C-H out-of-plane bending vibrations in benzene, thiophene benzotriazole and quinoxaline rings). The FT-IR spectra of PBZQ-2 and PBZQ-3 were basically the same as that of PBZQ-1 except for the slight difference in the peak intensities, which resulted from the different proportion of B, Z, Q units in the polymer backbones.

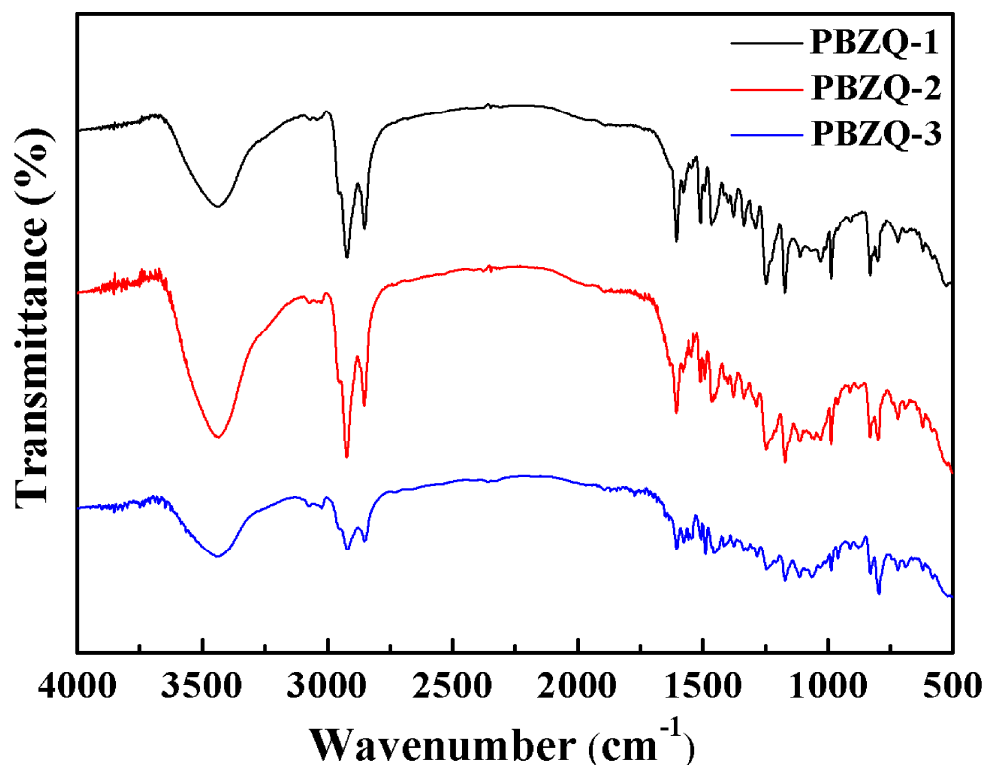


Fig. 1. FT-IR spectra of PBZQ-1, PBZQ-2 and PBZQ-3.

### 3.2. XPS characterization

The element composition of the polymer surface was analyzed by the XPS experiments to substantiate the constituent unit in the polymer backbone, and the spectra of C, N, O and S elements of PBZQ-1 were shown in Fig. 2. The C (1s) peak at 284.4 eV manifested the presence of  $sp^3$  hybridized carbon atoms which belonged to the alkyl and alkoxy chains in Z and Q units. The peak at 285.8 eV was derived from C-S (Z units) and C-O-C (Q units). C=N gave a peak at 287.1 eV for the C (1s). The N (1s) peak at 398.7 eV was originated from N=C in triazole and pyrazine (Z and Q units), and that at 401.6 eV was attributed to N-N in triazole (Z units). For the O (1s) spectrum, the peak at 532.3 eV corresponded to C-O-C, suggesting the existence of Q units in the polymer chain. The two S (2p) peaks centered at 163.5 eV ( $2p_{3/2}$ ) and 164.6 eV ( $2p_{1/2}$ ) were ascribed to thiophene-S, implying the presence of Z units in the polymer chain. Besides, the XPS spectra of PBZQ-2 and PBZQ-3 were also recorded (see supporting information Fig. S7 and Fig. S8), which presented the similar peaks as PBZQ-1 and confirmed the constitution of the polymers.

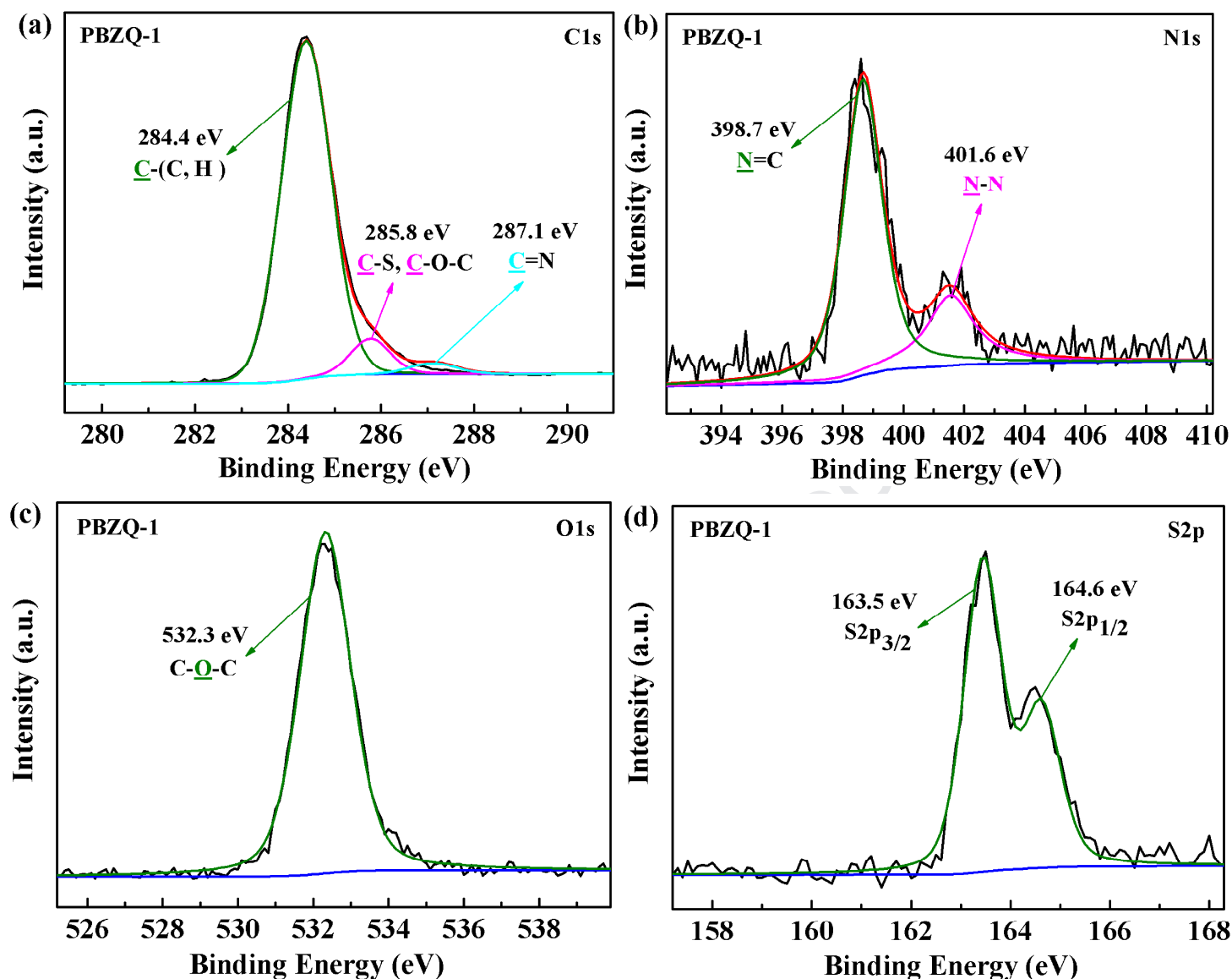


Fig. 2. XPS spectra of PBZQ-1: (a) C1s, (b) N1s, (c) O1s, and (d) S2p.

### 3.3. Electrochemical properties

After the polymers were sprayed onto the ITO glasses, the cyclic voltammetry (CV) experiments were carried out in ACN solution containing 0.1 M TBAPF<sub>6</sub> as supporting electrolyte at 100 mV/s scan rate to investigate their electrochemical properties, and the results were illustrated in Fig. 3. Besides, the CV measurements with 50 mV/s scan rate were also performed, and the redox peaks at 50 mV/s scan rate were similar with those at 100 mV/s scan rate (see supporting information Fig. S9). As shown in Fig. 3, all the three polymers exhibited obvious p-type doping process and the redox peaks were centered at 1.61 V/1.01 V for PBZQ-1, 1.57 V/1.00 V for

PBZQ-2 and 1.45 V/0.75 V for PBZQ-3. The onset oxidation potentials ( $E_{\text{onset}}$ ) of PBZQ-1, PBZQ-2 and PBZQ-3 were measured as 1.14 V, 1.13 V and 1.06 V, respectively. Both the oxidation peak potentials and  $E_{\text{onset}}$  displayed the same order as PBZQ-1 > PBZQ-2 > PBZQ-3, and especially the values of PBZQ-3 were obviously lower than those of PBZQ-1 and PBZQ-2, which resulted from the different proportions of the two acceptors (Z/Q) in the polymer backbones. By comparing the composition of the copolymer, it was easily found that PBZQ-1 possessed the highest content of Q units, followed by PBZQ-2 and PBZQ-3 in turn. The steric hindrance effect derived from the two (2-octyldodecyl)oxy groups in Q units would compel the adjacent rings to twist out of coplanarity, hence reduce the conjugated length and impede the transfer of donor electrons during the doping process [36]. As for Z units, the  $\pi$ -bridge flanking thiophene groups effectively strengthened the  $\pi$ - $\pi$  interaction and reduced the steric hindrance. On the other aspect, the thiophene groups, also as the electron rich donor units, would be beneficial to enhance the polymer highest occupied molecular orbital (HOMO) energy level, thus lowering the potential required for the formation of radical cation [37]. In summary, polymer with fewer Q units and more Z units presented the lower oxidation peak potential and  $E_{\text{onset}}$ .

In addition, it could be recognized from Fig. 3 that PBZQ-1 and PBZQ-2 did not show obvious n-type doping process, while PBZQ-3 possessed a slight n-type reduction peak at -0.45V which should be attributed to the high content of Z units in PBZQ-3 backbone as benzotriazole-based polymers usually displayed double-doping features (p-type and n-type doping) [23]. For most polymers, the presence of dissolved oxygen and little water in the electrolyte solution will make it difficult for the inherently unstable n-type doping to exist.

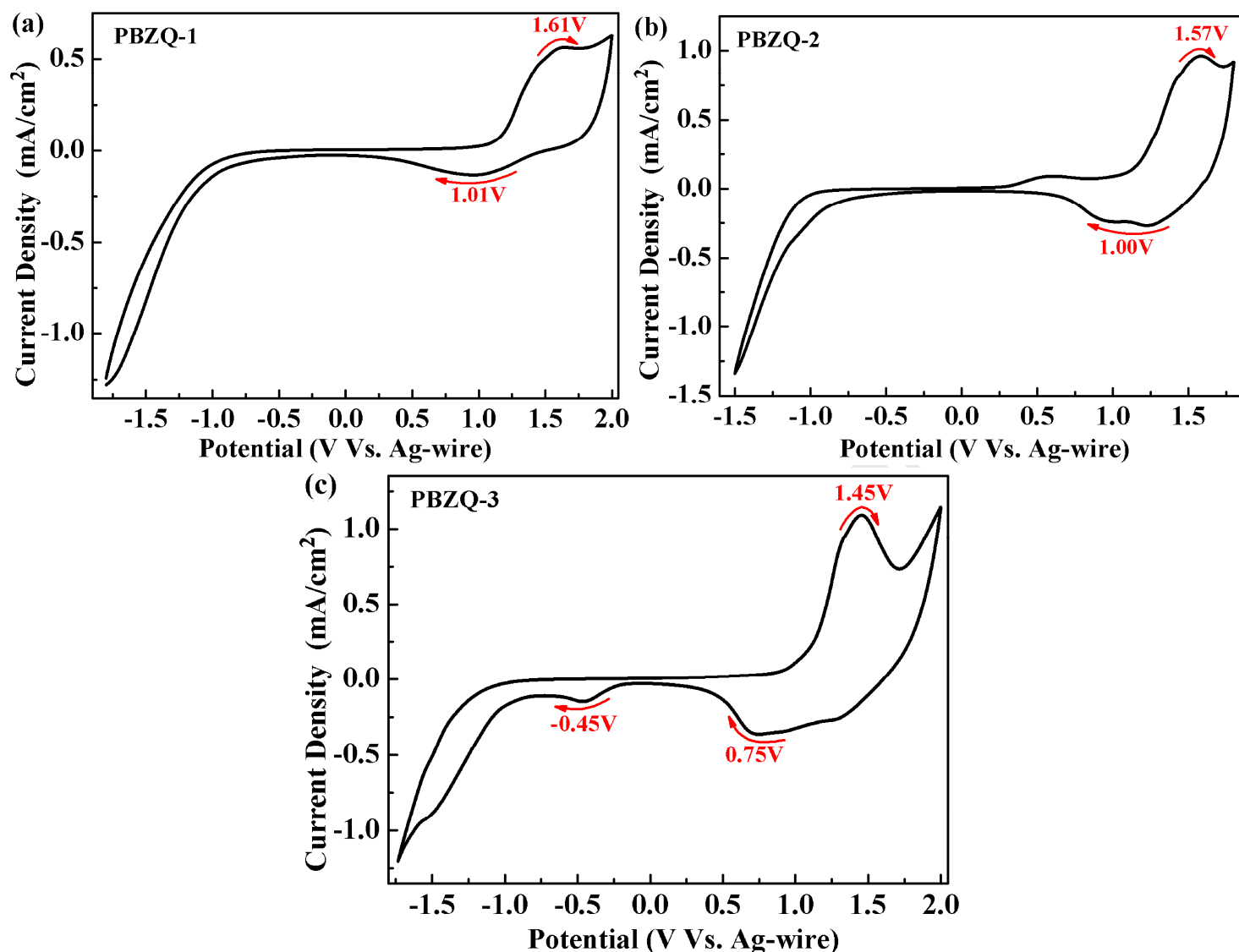


Fig. 3. CV curves of the polymer films: (a) PBZQ-1, (b) PBZQ-2, and (c) PBZQ-3.

### 3.4. Optical properties

The UV-Vis absorption spectra of the three polymers in the liquid state (dissolved in DCM) and in the solid state (spray-coated on ITO electrodes and de-doped) were examined and analyzed. As shown in Fig. 4, each polymer in the different phase state revealed the similar spectra with two absorption peaks which stemmed from the high energy and the low energy  $\pi$ - $\pi^*$  transitions [38]. In the DCM solution, the maximum absorption wavelengths ( $\lambda_{\max}$ ) were 398 nm/485 nm for PBZQ-1, 397 nm/484 nm for PBZQ-2 and 520 nm/561 nm for PBZQ-3, as well as in the solid film, the  $\lambda_{\max}$  were 403 nm/492 nm for PBZQ-1, 403 nm/491 nm for PBZQ-2 and 521 nm/561 nm for PBZQ-3. It could be observed that the  $\lambda_{\max}$  of the



three polymers in the solid state exhibited small bathochromic shifts compared with those in the solution state which suggested the solid films possessed the improved  $\pi$ - $\pi^*$  stacking and stronger intra molecular interaction [39,40].

By comparing among the three polymers, both in the solution and in the solid film, PBZQ-1 and PBZQ-2 displayed essentially the same absorption peaks and had obvious hypsochromic shifts in contrast with PBZQ-3. In general, quinoxaline possessed the stronger electron-accepting ability and bandgap-lowering ability than benzotriazole [41], but in the main chains of PBZQ-1 and PBZQ-2, the more content Q units with the alkoxybenzene substitutions caused the larger steric hindrance between (2-octyldodecyl)oxy and adjacent units which offset the powerful electron-withdrawing effect of quinoxaline [36]. In addition, as mentioned earlier, the larger proportion of Z units in PBZQ-3 backbone carried more thiophene groups arranged on both sides of benzotriazole, which could availably reduce the steric hindrance between Z and benzene/Q units, as well as improve the planarity and D-A conjugation of the polymer chains [32]. Thus, the UV-Vis absorption spectra of PBZQ-3 showed bathochromic shifts compared with those of PBZQ-1 and PBZQ-2. Besides, corresponding to the absorption bands in the visible region, PBZQ-1 and PBZQ-2 showed orange-red color both in liquid and solid phases, while PBZQ-3 displayed strawberry red in the solution and tomato red in the solid film.

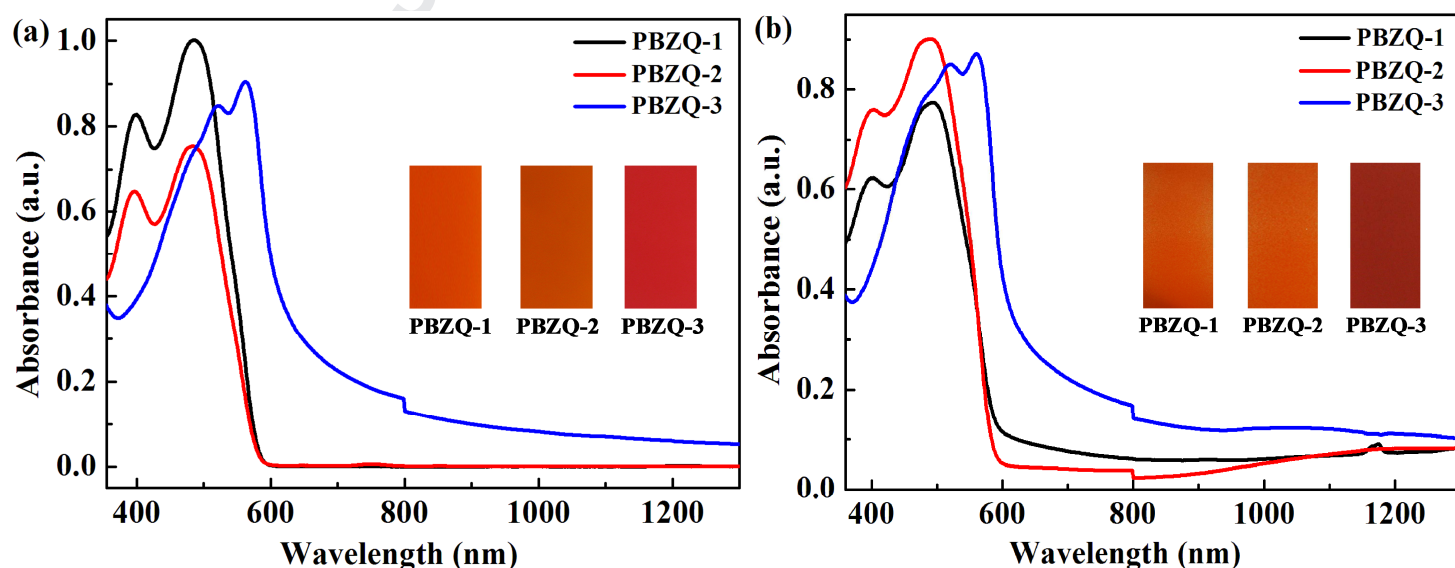


Fig. 4. UV-Vis absorption spectra of PBZQ-1, PBZQ-2 and PBZQ-3: (a) in solution and (b) in

solid films.

### 3.5. Spectroelectrochemical properties

Spectroelectrochemistry is a useful method for studying the optical changes in the absorption spectra and gaining the information about the electronic structures of conjugated polymers as a function of the applied potential difference. After the polymers were spray-coated onto the ITO glasses, the spectroelectrochemical experiments were performed in a 0.1 M TBAPF<sub>6</sub>/ACN solution with applied potentials ranging from 0 V to 1.5 V. Fig. 5 revealed the absorption spectra and the corresponding colors of the three polymer films in the neutral and doped states.

As shown in Fig. 5, PBZQ-1, PBZQ-2 and PBZQ-3 exhibited two absorption peaks in the neutral states due to the  $\pi$ - $\pi^*$  transitions in the polymer main chains, which accorded with the feature of D-A type conjugated polymers [42]. And the absorption peaks were regarded as the transitions from benzene and thiophene based valence bands to their antibonding counterparts (high-energy transition) and to the substituent localized narrow conduction bands (low-energy transition) [43]. The peaks were located at 403 nm/492 nm for PBZQ-1, 403 nm/491 nm for PBZQ-2 and 521 nm/561 nm for PBZQ-3, which made their color manifest orange-red for PBZQ-1 and PBZQ-2, and red for PBZQ-3 in the neutral states (0 V).

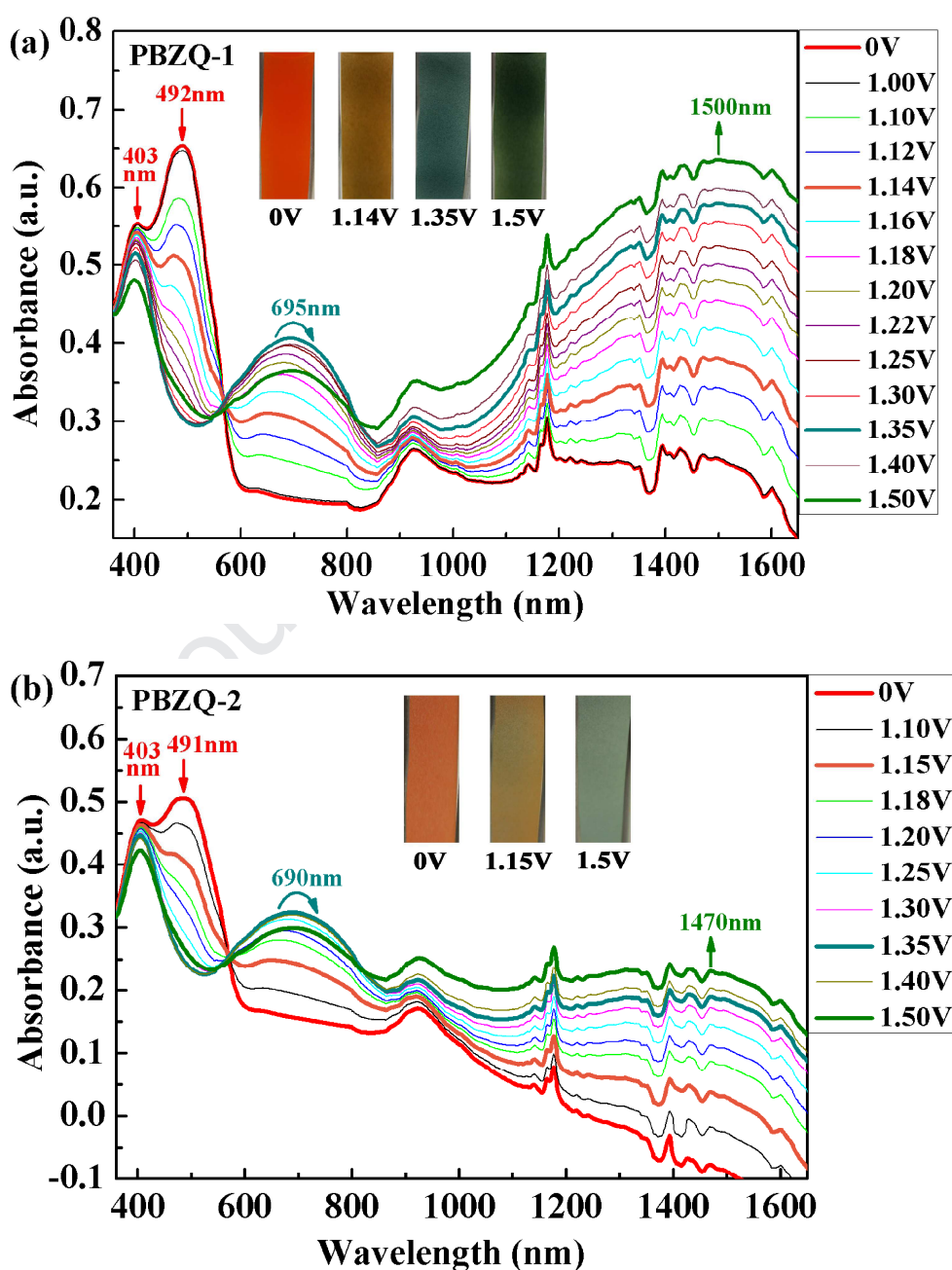
As the potentials continued to increase irregularly, the absorption spectra of the three polymers demonstrated the similar changes. It could be observed from Fig. 5a that the two absorption peaks of PBZQ-1 in the neutral state declined gradually, especially the absorption band at 492 nm vanished when the potential reached 1.25 V. Meanwhile, the other two new absorption bands centered at 695 nm and 1500 nm emerged and heightened, which corresponded to the formations of polarons and bipolarons respectively. The absorption peak located at 695 nm reached its maximum at 1.35 V, and then decreased gradually as the oxidation continued. The other peak in the near infrared region around at 1500 nm enhanced continually with the augment of applied potential until PBZQ-1 was completely oxidized at 1.5 V. The decline of polaron band from 1.35 V to 1.5 V could be explained that the successively improving

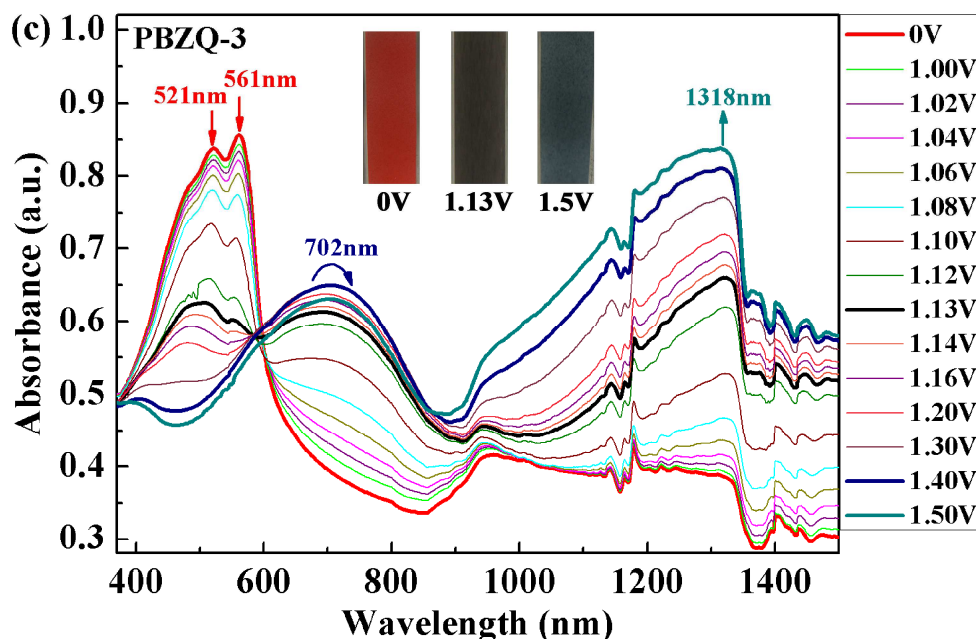
bipolaron band (around 1500 nm) restrained the polaronic population which was also called the repression of interband transition [44]. Some other polymers also demonstrate the similar phenomenon that is they would lead to spin-1/2 polarons at light doping and blossom into spinless bipolarons at heavy doping [29,45]. Moreover, the gradually weakened  $\pi$ - $\pi^*$  transition bands and the significantly enhanced polaron band were both situated in the visible region, so PBZQ-1 exhibited several different colors in the oxidation process as observed in Fig. 5a. Upon stepwise oxidation, the neutral orange-red (0 V) PBZQ-1 changed to brown-yellow at 1.14 V, cyan at 1.35 V, and green at 1.5 V in turn. It was clear that PBZQ-1 showed multichromism and the color changes covered red, yellow, cyan and green, in which red and green belonged to the RGB colors. As previously mentioned, multichromic polymers have important application values in smart window and optical display technology [5,6,46], and particularly, the multicolor polymers with green color and good solubility are rarely reported in the literatures [7,8,47]. Therefore, the design and synthesis of PBZQ-1 had great significance for the development of electrochromic polymers.

As the oxidation degree of PBZQ-2 raised (Fig. 5b), the two  $\pi$ - $\pi^*$  transition peaks weakened gradually and the peak at 491 nm disappeared absolutely at 1.25 V. At the same time, the polaron band at 690 nm enhanced to maximum at 1.35 V, and the bipolaron band at about 1470 nm steadily increased until 1.50 V. The color changes of PBZQ-2 were from orange-red (0 V), to yellow (1.15 V), and to light grass green (1.5 V) which illustrated in Fig. 5b.

During the oxidation process of PBZQ-3 as Fig. 5c suggested, the peaks at 521 nm and 561 nm attenuated gradually until both of them faded away at 1.30 V. While the polaron band at 702 nm improved to the maximum at 1.40 V and then decreased, and the bipolaron band at 1318 nm maintained the trend of growth with the increase of the applied potentials. It was noteworthy that when PBZQ-3 was oxidized to 1.13 V, its absorption band uniformly covered the entire visible region between 400 nm and 760 nm, which indicated that PBZQ-3 displayed black color. At the potential of 1.5 V for complete oxidation, the only absorption peak of 702 nm in the visible region made PBZQ-3 show grey-blue color. As shown in Fig. 5c, PBZQ-3 underwent red

(0V), black (1.13V) and grey-blue (1.5 V) with the increase of applied potentials as expected. A polymer owning black color in any state is very important in the application of smart window [21]. In consideration of the difficulty in gaining black color, PBZQ-3 offered a new kind of structure design for black electrochromic polymer and deserved further research and development [9,48]. From the above analysis of PBZQ-1, PBZQ-2 and PBZQ-3, it was concluded that adjusting the proportion of the two acceptors was a useful method to tailor the polymer color.








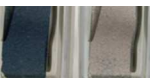


**Fig. 5.** Spectroelectrochemical spectra of the polymer films and their color changes at different applied potentials: (a) PBZQ-1, (b) PBZQ-2, and (c) PBZQ-3.

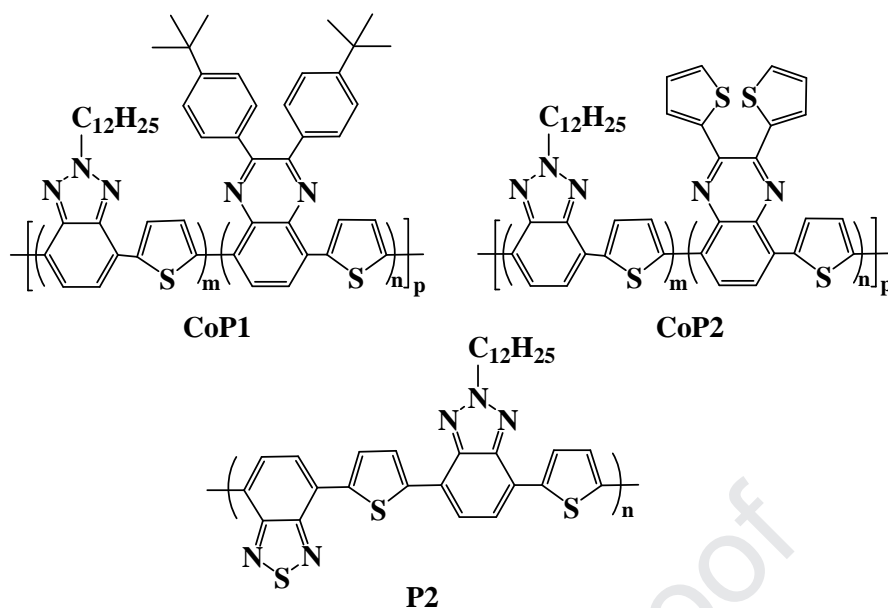
In addition, some electrochemical and optical parameters of the polymers such as the  $\lambda_{\text{max}}$  in the liquid state and in the solid state, the onset wavelengths of the optical absorption spectra in the neutral states ( $\lambda_{\text{onset}}$ ), the  $E_{\text{onset}}$ , the optical band gaps ( $E_{\text{g,op}}$ ), and the HOMO/LUMO values were all illustrated in Table 1. The  $\lambda_{\text{onset}}$  of PBZQ-1, PBZQ-2 and PBZQ-3 films were 588 nm, 593 nm and 624 nm, and the  $E_{\text{g,op}}$  of them were calculated as 2.11 eV, 2.09 eV and 1.99 eV, respectively. The order of  $E_{\text{g,op}}$  was PBZQ-1 > PBZQ-2 > PBZQ-3, which was due to the gradually incremental molar ratio of Z units to Q units in the polymer backbones. As previously discussed, the two thiophene groups connected on benzotriazole improved the electron-accepting ability of Z units, but the long-chain alkoxy substitutions adjacent to quinoxaline diminished the electron-accepting ability of Q units [32,36,41]. Consequently, the  $E_{\text{g,op}}$  of polymers decreased gradually with the increase of Z unit content, which could also be reflected by the HOMO and LUMO energy levels. PBZQ-3 had the largest molar ratio of Z to Q (4:1) in contrast with PBZQ-1 (1:2) and PBZQ-2 (1:1), which not only made the polymer have the most donor units (thiophene groups were also regarded as donors) and hence show the highest HOMO energy level, but also made the polymer have the most Z acceptor units with stronger electron-deficient ability and thus

display the lowest LUMO energy level [37]. Besides, the other three copolymers based on benzotriazole and quinoxaline units reported in the literatures were compared with PBZQ-1, PBZQ-2 and PBZQ-3, and their molecular structures were shown in Fig. 6 [49,50]. As list in Table 1, CoP1, CoP2 and P2 displayed two colors in the redox process, though they had the relatively lower  $E_{g,op}$ . PBZQ-1, PBZQ-2 and PBZQ-3 exhibited impressive multicolor, and the more alkyl side chains caused higher  $E_{g,op}$ , but also increased the solubility of polymers.

**Table 1** Electrochemical and optical parameters of PBZQ-1, PBZQ-2, PBZQ-3, and several other copolymers with similar structures.

Polymer	$\lambda_{max}$ (solution) nm	$\lambda_{max}$ (film) nm	$\lambda_{onset}$ (film) nm	$E_{onset}$ V	$E_{g,op}^a$ eV	HOMO <sup>b</sup> eV	LUMO <sup>c</sup> eV	color
PBZQ-1	398/485	403/492	588	1.14	2.11	-5.54	-3.43	
PBZQ-2	397/484	403/491	593	1.13	2.09	-5.53	-3.44	
PBZQ-3	520/561	521/561	624	1.06	1.99	-5.46	-3.47	
CoP1 <sup>d</sup>	-	-	-	-	1.72	-5.22	-3.55	
CoP2 <sup>d</sup>	-	-	-	-	1.48	-5.41	-3.65	
P2 <sup>e</sup>	-	-	-		1.62	-5.67	-3.55	

<sup>a</sup>  $E_{g,op} = 1241/\lambda_{onset}$ ; <sup>b</sup>  $E_{HOMO} = -e(E_{onset} + 4.4)$ ; <sup>c</sup>  $E_{LUMO} = E_{HOMO} + E_{g,op}$ ; <sup>d</sup> Data were taken from reference [49]; <sup>e</sup> Data were taken from reference [50].



**Fig. 6.** Molecular structures of the polymers reported in the literatures.

### 3.6. Electrochromic switching properties

In order to study the kinetic properties of polymers, electrochromic switching tests were carried out using the double potential step chronoamperometry technique. The polymers were sprayed onto the ITO glasses beforehand, and then the experiments were performed in ACN solution containing 0.1 M TBAPF<sub>6</sub> electrolyte under the repeated potential stepping between reduced and oxidized states with a residence time of 4 s. The average thicknesses of PBZQ-1, PBZQ-2 and PBZQ-3 films were estimated as 348 nm, 381 nm and 378 nm, respectively. The kinetic curves and the calculated kinetic parameters at the definite wavelengths were manifested in Fig. 7-9, Fig. S10-S12, Fig. S13-S15 (in supporting information) and Table 2 respectively.

Optical contrast ( $\Delta T\%$ ) refers to the percentage transmittance change between oxidized and neutral states, and the  $\Delta T\%$  values of PBZQ-1 at 490 nm, 690 nm and 1500 nm were 28.4% (Fig. 7a), 27.2% (Fig. 8a) and 38.9% (Fig. 9a) respectively. While the  $\Delta T\%$  values of PBZQ-2 at 490 nm, 690 nm and 1500 nm were 21.1%, 36.8% and 41.5% respectively (see supporting information Fig. S10-S12), and those of PBZQ-3 at 520 nm, 720 nm and 1320 nm were 20.6%, 22.8% and 33.7% respectively (see supporting information Fig. S13-S15). From the data it was found



that all the three polymers exhibited higher  $\Delta T\%$  in the near-infrared region compared with in the visible region, which was in agreement with many D-A type electrochromic polymers [8]. In addition, by contrasting the three polymers, PBZQ-1 and PBZQ-2, which possessed more Q units connected with more (2-octyldodecyl)oxy groups, revealed relatively higher  $\Delta T\%$  than PBZQ-3 at all corresponding wavelengths. The long-chain alkoxy groups could expand the distance of chain segments and improve the charge/discharge capacity in the redox process, thus raising the optical transmittance to a certain degree [51].

Switching time ( $t_{95\%}$ ) is defined as the time required for reaching 95% of the maximum transmittance change between bleached and colored states, and this value can represent the switching speed of the polymer. As listed in Table 2, the  $t_{95\%}$  of PBZQ-1 at 490 nm, 690 nm and 1500nm were 3.39 s, 1.70 s and 2.46 s, the  $t_{95\%}$  of PBZQ-2 at 490 nm, 690 nm and 1500nm were 3.61 s, 2.04 s and 2.12 s, and the  $t_{95\%}$  of PBZQ-3 at 520 nm, 720 nm and 1320nm were 3.00 s, 0.91 s and 1.81 s. Except at the wavelengths of high energy absorption peaks, the  $t_{95\%}$  values of the three polymers at other wavelengths were less than 3 s. And in contrast to PBZQ-3, PBZQ-1 and PBZQ-2 showed the longer response time at the corresponding wavelengths, which also resulted from the more Q units with more long-chain alkoxy groups in their backbones.

Coloration efficiency (CE) denotes the ratio between optical density change ( $\Delta OD$ ) and charge consumed per unit electrode area ( $\Delta Q$ ), which can be used to evaluate the polymer power efficiency during the electrochromic switching process. The formula was shown below [52]:

$$CE = \frac{\Delta OD}{\Delta Q}$$

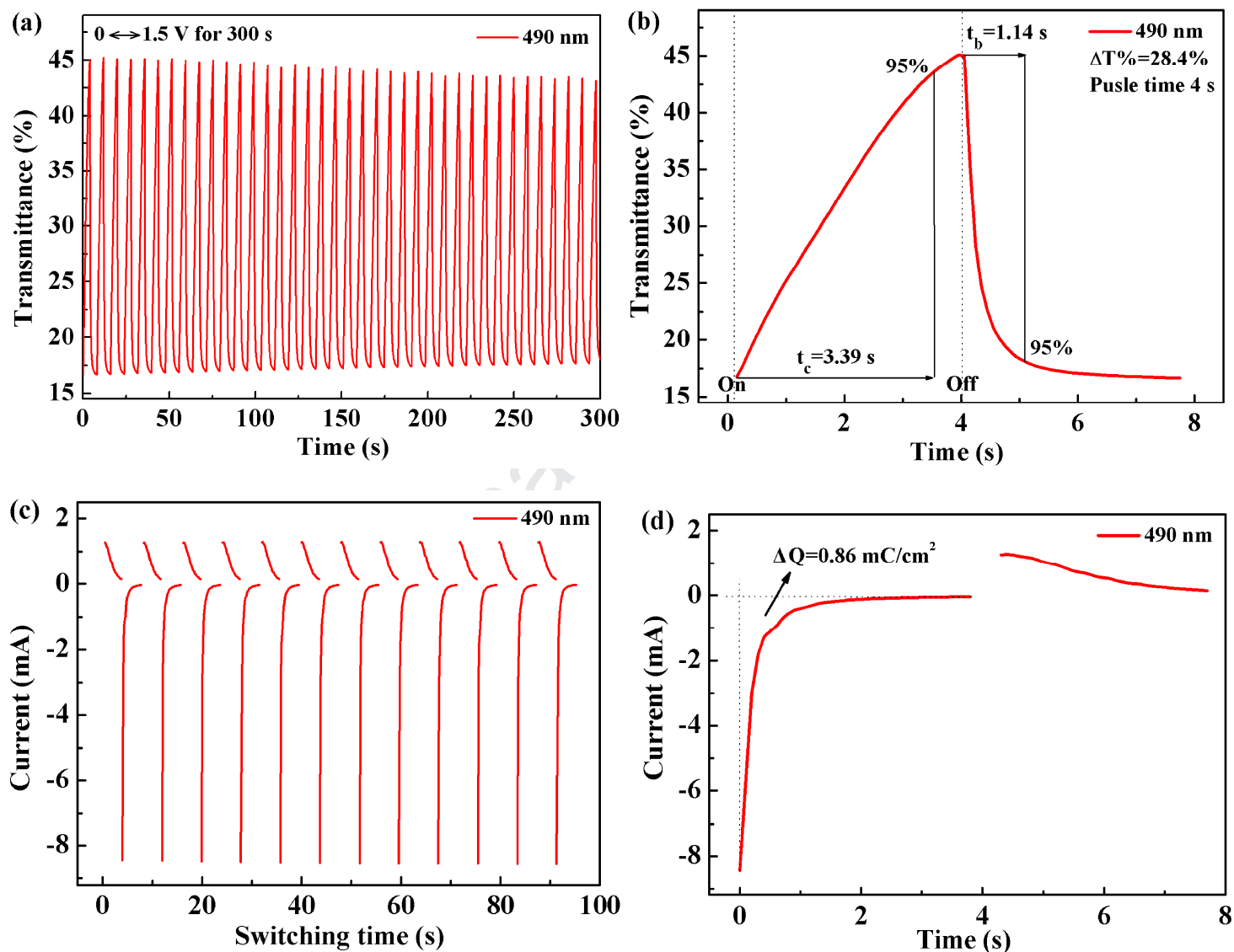
$$\Delta OD = \log \left( \frac{T_b}{T_c} \right)$$

$$\Delta Q = \frac{Q}{A}$$

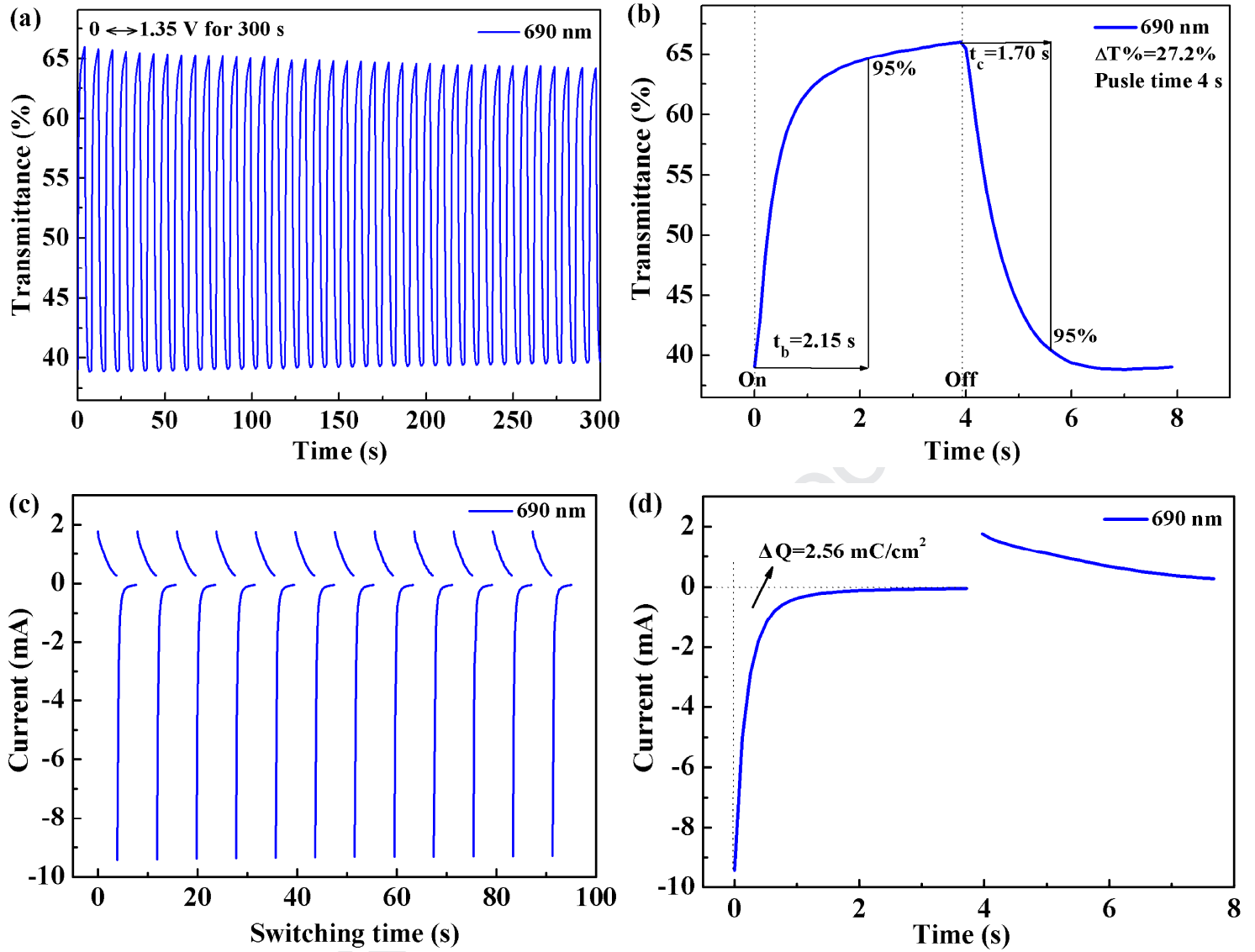
Wherein,  $T_b$  and  $T_c$  are the transmittance in the bleaching state (neutral state) and



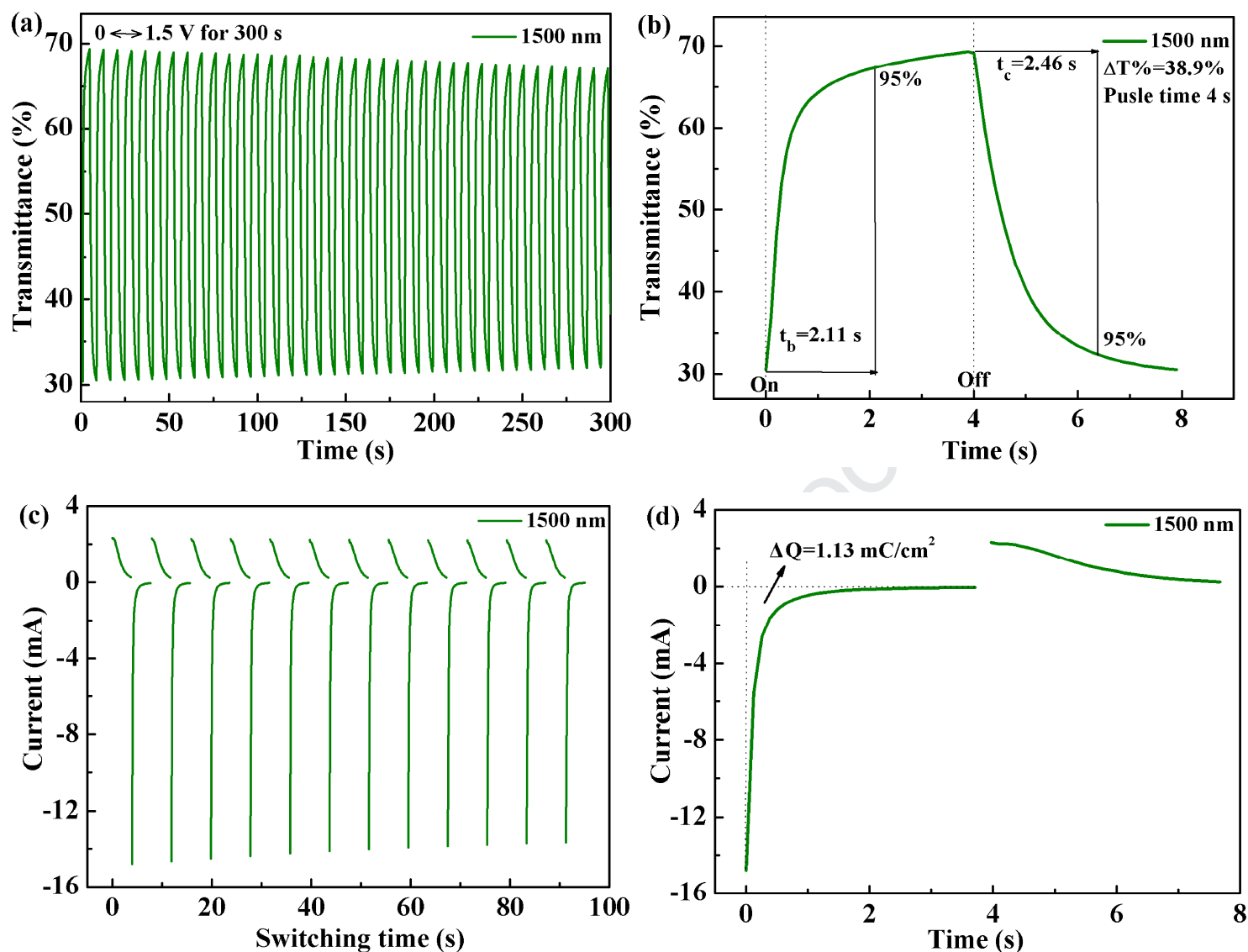
in the colored state (oxidation state).  $Q$  is the total charge acquired by integrating of the multi-potential step curve.  $A$  is the effective area of ITO glass. As shown in Table 2, all the polymers demonstrated the relatively larger CE values, and in particular, PBZQ-1 deserved focused attention with a CE value as high as  $498.26 \text{ cm}^2/\text{C}$  at 490 nm. In conclusion, the three polymers displayed satisfactory kinetic performances which also could be adjusted through optimizing Z-to-Q proportion.



**Fig. 7.** (a) Transmittance-time curve of PBZQ-1 at 490 nm. (b) The coloring time ( $t_c$ ) and the bleaching time ( $t_b$ ) of PBZQ-1 at 490 nm. (c) Current-switching time curve of PBZQ-1 between 0 V and 1.5 V at 490 nm. (d) Charge density consumed during the dedoping process at 490 nm.



**Fig. 8.** (a) Transmittance-time curve of PBZQ-1 at 690 nm. (b) The coloring time ( $t_c$ ) and the bleaching time ( $t_b$ ) of PBZQ-1 at 690 nm. (c) Current-switching time curve of PBZQ-1 between 0 V and 1.35 V at 690 nm. (d) Charge density consumed during the dedoping process at 690 nm.



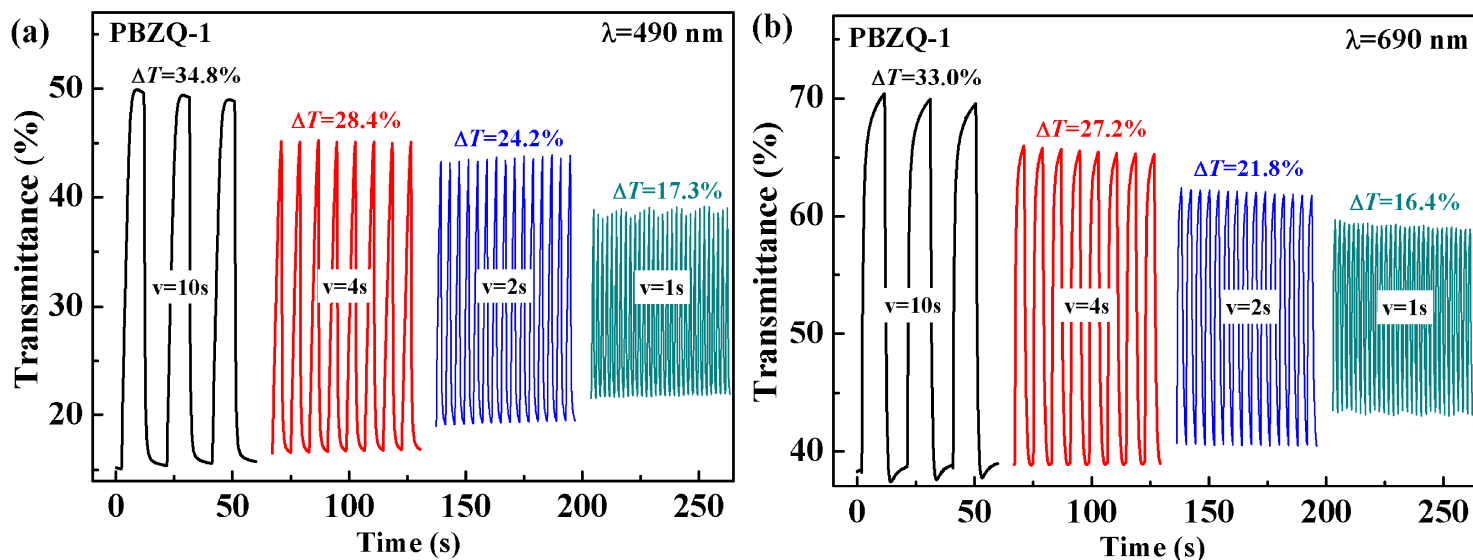
**Fig. 9.** (a) Transmittance-time curve of PBZQ-1 at 1500 nm. (b) The coloring time ( $t_c$ ) and the bleaching time ( $t_b$ ) of PBZQ-1 at 1500 nm. (c) Current-switching time curve of PBZQ-1 between 0 V and 1.5 V at 1500 nm. (d) Charge density consumed during the dedoping process at 1500 nm.

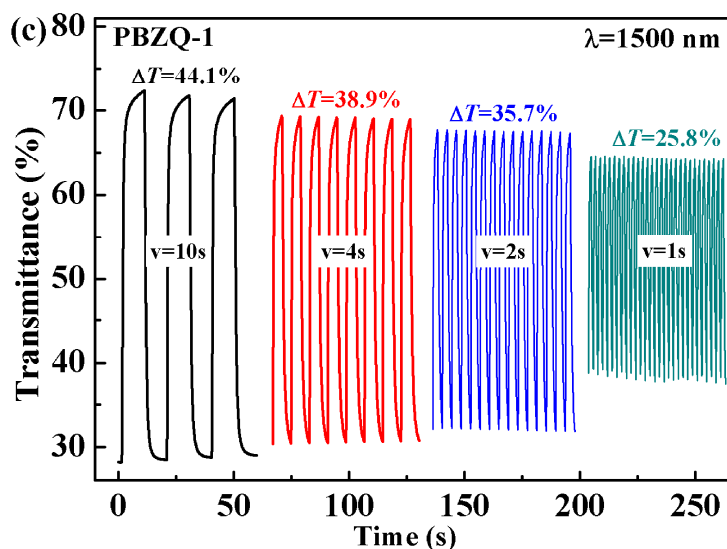
**Table 2** The  $\Delta T\%$ ,  $t_{95\%}$  and CE values of the polymers at different wavelengths.

Polymer	$\lambda$ nm	$\Delta T\%$ %	$t_{95\%}$ s	CE $\text{cm}^2/\text{C}$
PBZQ-1	490	28.4	3.39	498.26
	690	27.2	1.70	237.50
	1500	38.9	2.46	316.8
PBZQ-2	490	21.1	3.61	291.50

	690	36.8	2.04	206.62
	1500	41.5	2.12	359.37
	520	20.6	3.00	262.40
PBZQ-3	720	22.8	0.91	155.08
	1320	33.7	1.81	122.83

Furthermore, for studying the effect of different residence time on the performance of electrochromic switching, the  $\Delta T\%$  of the polymers were detected at the residence times of 10 s, 4 s, 2s and 1 s respectively. As shown in Fig. 10, when the retention time decreased from 10s to 1s, the  $\Delta T\%$  of PBZQ-1 declined by 17.5% at 490 nm, 16.6% at 690 nm and 18.3% at 1500 nm. The  $\Delta T\%$  of PBZQ-2 reduced by 30.1% at 490 nm, 33.6 % at 690 nm and 35.8% at 1500 nm, and the  $\Delta T\%$  of PBZQ-3 declined by 11.5% at 520 nm, 21.1% at 720 nm and 28.2% at 1320 nm (see supporting information Fig. S16). It was easy to find that the  $\Delta T\%$  of the three polymers all expressed obvious attenuation with the decreasing of residence time which was due to the fact that the polymer could not be fully doped (oxidized) or dedoped (reduced) when the retention time was short.





**Fig. 10.** Electrochromic switching of PBZQ-1 with interval of 10 s, 4 s, 2 s and 1 s: (a) 490 nm, (b) 690 nm, and (c) 1500 nm.

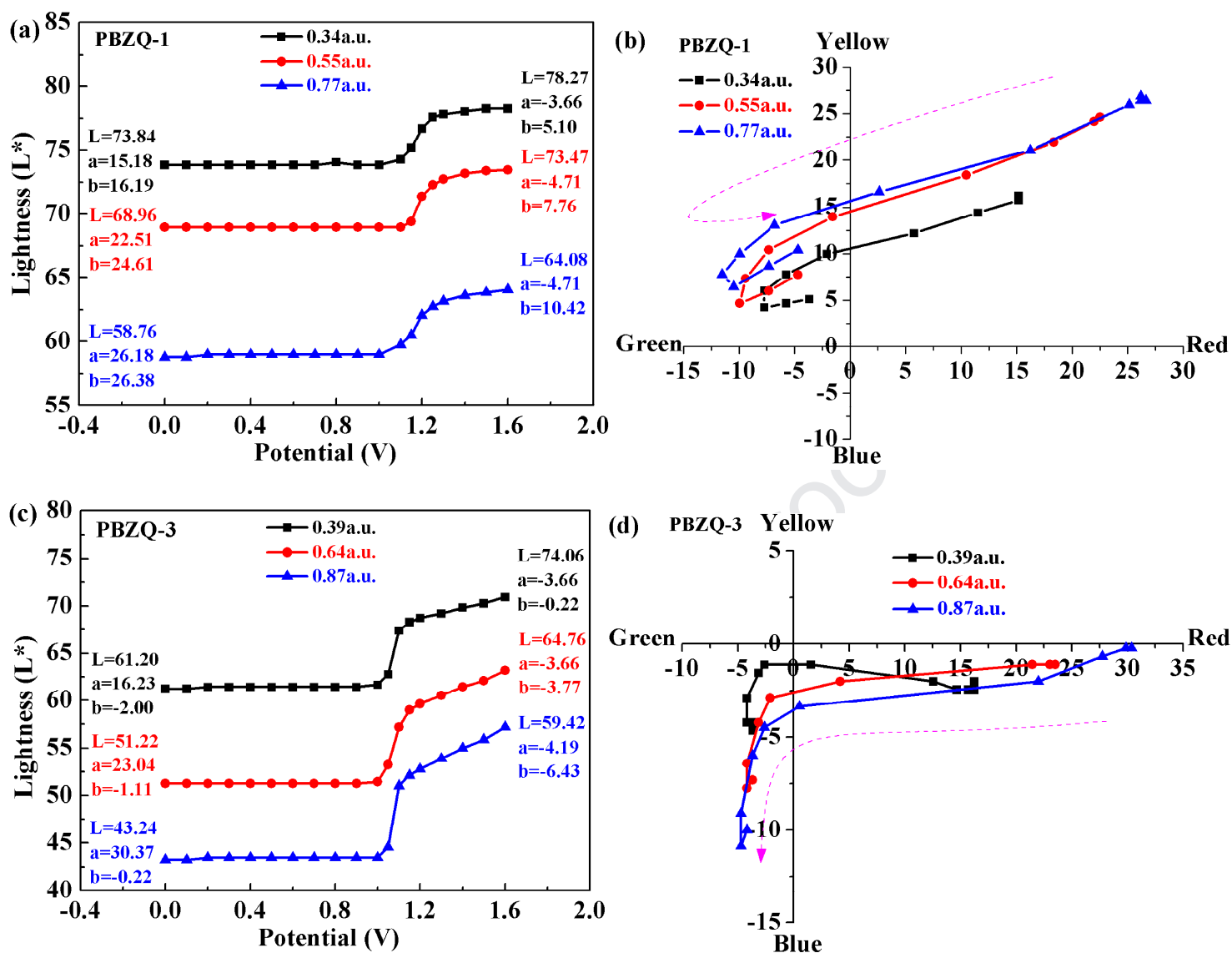
### 3.7. Colorimetry

Based on the spectroelectrochemical experiments, it was observed that the color changes of the three polymer films were obviously different during the oxidation-reduction process. If we want to investigate the color changes in depth, however, the first one to be used was CIE 1976  $L^*a^*b^*$  Color Space to detect the variations of lightness, chroma and hue of the polymers, in which  $L^*$  denotes the luminance of color from black to white,  $a^*$  denotes red-green balance, and  $b^*$  denotes yellow-blue balance [24,48]. The  $L^*$ ,  $a^*$ , and  $b^*$  values of the polymer films with different thicknesses (represented by the maximum optical absorption values) were determined by spectrophotometer at the scanning potential from 0 to 1.6 V, and the data were depicted in Fig. 11 and Fig. S17 (in supporting information).

As shown in Fig. 11a, regardless of the thickness of PBZQ-1, the  $L^*$  values had the same change trend with the raise of the applied potentials. Starting from 0 V, the  $L^*$  values remained unchanged until the potential exceeded the  $E_{\text{onset}}$ , and then began to augment by degrees. On the other aspect, at the same applied potential, with the thickness of PBZQ-1 increased, that is, the maximum optical absorption value increased from 0.34a.u to 0.55a.u., and to 0.77a.u., its  $L^*$  values decreased gradually. The thicker the polymer film was, the lower intensity the light passed through, which

caused the weakening of the luminance and the decline of the  $L^*$  value. Besides, it was found that PBZQ-2 (see supporting information Fig. S17a) and PBZQ-3 (Fig. 11c) exhibited the similar tendency on the  $L^*$  values as PBZQ-1.

In the  $a^*$ - $b^*$  graphs of PBZQ-1, as demonstrated in Fig. 11b, the  $a^*$  values changed from positive to negative with the color changing from red to green with the steady increasing of applied potentials, and meanwhile, the  $b^*$  values always changed in positive range with the yellow component. The  $a^*$ - $b^*$  curves gradually declined and rebounded to a certain extent from the first quadrant to the second quadrant. This tendency was consistent with the conclusion of spectroelectrochemical experiments with the color transformations from orange-red to brown-yellow, to cyan, and to green in the process of polymer oxidation. In particular, it was observed from the spectroelectrochemical spectra (Fig. 5a) that the peak intensities of PBZQ-1 in the red and blue regions (at 403 nm and 695 nm) at 1.35 V were both higher than those at 1.50 V, which corresponded to the inflection points in the  $a^*$ - $b^*$  curves (Fig. 11b), that is, PBZQ-1 had more green color component when oxidized to 1.35 V. For PBZQ-2 (see supporting information Fig. S17b), the change of  $a^*$  and  $b^*$  values was similar with PBZQ-1, and the overall trend of  $a^*$ - $b^*$  curves also changed from the first quadrant to the second quadrant with the color changes from orange-red, to yellow, and to light grass green as the applied potential increasing. When it came to PBZQ-3 (Fig. 11d), the  $a^*$  values changed from positive to negative with the applied potentials raising, but the  $b^*$  values varied in negative range with the blue component. The overall trend of  $a^*$ - $b^*$  changed from the fourth quadrant to the third quadrant accompanied by the color changes from red to black, and to grey-blue. Significantly, the  $a^*$  and  $b^*$  values were close to 0 at the intermediate potentials, especially a set of  $a^*/b^*$  values was measured as 0.52/-3.32 at the maximum optical absorption value 0.87 a.u., the closest to an achromic black accompanying with the corresponding low  $L^*$  value.



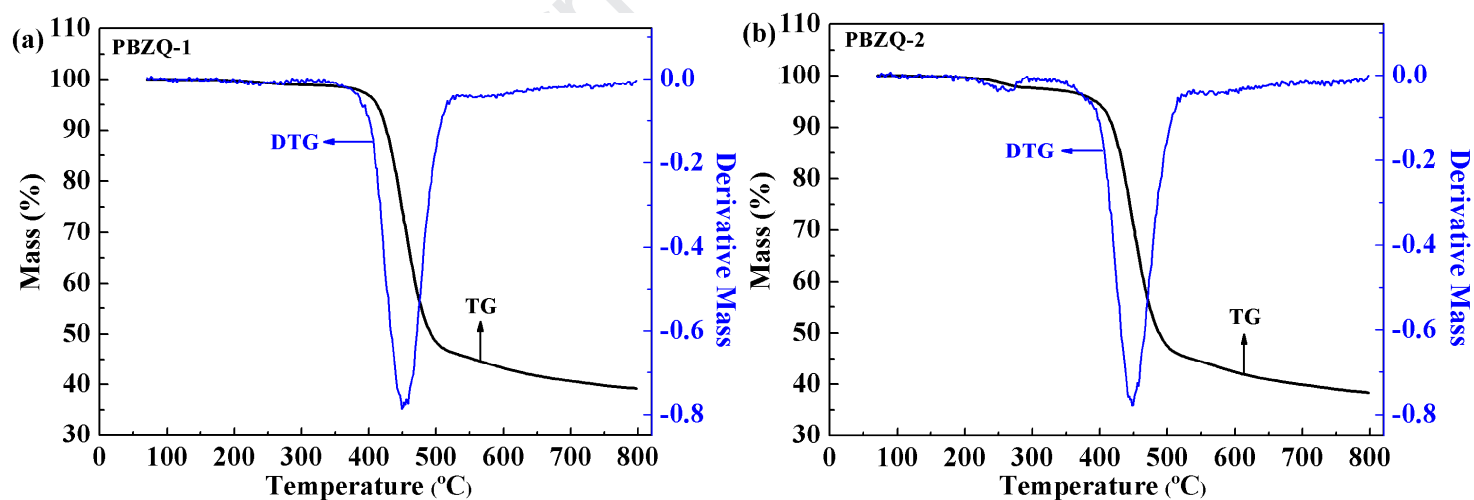
**Fig 11.** The  $L^*$  and  $a^*-b^*$  graphs of the polymers at different potentials. (a) The changes in  $L^*$  of PBZQ-1, (b) the changes in  $a^*-b^*$  of PBZQ-1, (c) the changes in  $L^*$  of PBZQ-3, and (d) the changes in  $a^*-b^*$  of PBZQ-3.

### 3.8. Thermogravimetric analysis

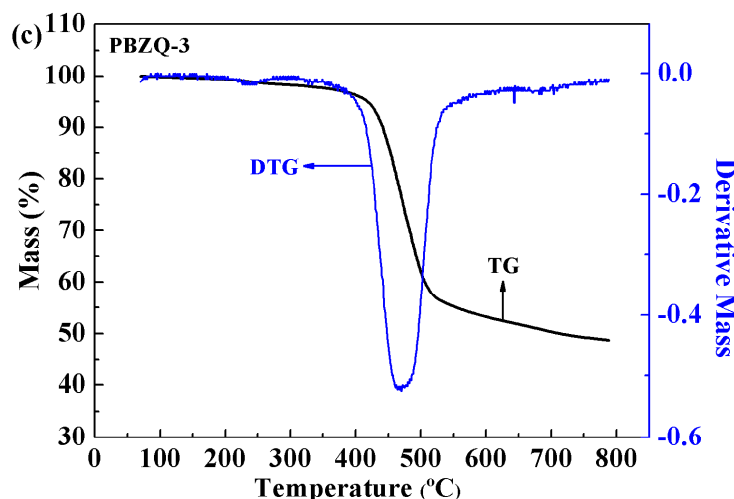
Thermogravimetric analysis is a simple and effective method to evaluate the polymer thermal stability [29,53]. Fig. 12 showed the thermogravimetric (TG) and differential thermal gravity (DTG) curves of the polymers with the heating rate of 15 °C/min.

It was found from TG curve of PBZQ-1 (Fig. 12a) that it displayed significant decomposition between 412.4 °C (extrapolated onset temperature,  $T_{onset}$ ) and 491.6 °C

(extrapolated termination temperature,  $T_{\text{offset}}$ ). Similarly, the  $T_{\text{onset}}/T_{\text{offset}}$  of PBZQ-2 and PBZQ-3 were measured as 413.8 °C/495.8 °C and 423.5 °C/ 511.5 °C respectively based on Fig. 12b and Fig. 12c. And the decomposition temperature at 5% weight loss ( $T_d$ ) were 412.0 °C, 394.2 °C and 418.5 °C for PBZQ-1, PBZQ-2 and PBZQ-3. In addition, from the DTG curves, every polymer expressed only one peak corresponding to the temperature with maximum degradation rate ( $T_{\text{max}}$ ). The specific values were measured as 449.3 °C for PBZQ-1, as 449.3 °C for PBZQ-2, and as 470.0 °C for PBZQ-3. The rapid mass loss was attributed to the decomposition of majority of the copolymers' branches and part of their main chains. The amounts of carbonized residue, also known as char yields (% char), were 39.8% for PBZQ-1, 39.0% for PBZQ-2, and 49.2% for PBZQ-3 at 750 °C, which was ascribed to a large number of aromatic groups distributed in the polymer backbones. The above parameters including  $T_{\text{onset}}$ ,  $T_{\text{offset}}$ ,  $T_d$ ,  $T_{\text{max}}$  and % char were all listed in Table 3, and these data suggested that all the three polymers manifested favorable thermal stability, especially PBZQ-3, which was helpful to improve the service time of electrochromic devices in practical application.







**Fig. 12.** The TG and DTG curves of the polymers: (a) PBZQ-1, (b) PBZQ-2, and (c) PBZQ-3.

**Table 3** The TG parameters of the polymers.

Polymers	T <sub>onset</sub> (°C)	T <sub>offset</sub> (°C)	T <sub>d</sub> (°C)	T <sub>max</sub> (°C)	% char
PBZQ-1	412.4	491.6	412.0	449.3	39.8
PBZQ-2	413.8	495.8	394.2	449.3	39.0
PBZQ-3	423.5	511.5	418.5	470.0	49.2

#### 4. Conclusion

In this work, three medium-bandgap soluble copolymers employing alternate benzotriazole and quinoxaline groups as acceptors, namely PBZQ-1, PBZQ-2 and PBZQ-3, were synthesized successfully. The different feed ratio of acceptor units in the three polymers led to the diverse electrochromic properties which were mainly manifested in the electrochemical, optical and colorimetric performances. Significantly, they all underwent several distinct colors during the oxidation process, i.e., PBZQ-1 showed orange-red, brown-yellow, cyan and green, PBZQ-2 exhibited orange-red, yellow and light grass green, as well as PBZQ-3 displayed red, black and grey-blue. Besides, the three polymers presented satisfactory thermal stability and kinetic properties such as the relatively high optical contrast, the short switching time and the attractive coloration efficiency. In summary, each polymer demonstrated the individually distinguishing character, and the most remarkable feature was their multichromism including RGB and black colors, which made it possible for the three copolymers to become electrochromic materials with commercial application

prospects.

## Acknowledgements

The work was financially supported by the Natural Science Foundation of Shandong Province (ZR2019MEM031), and the National Natural Science Foundation of China (51473074, 21601079).

## Appendix A. Supporting Information

Supplementary data to this article were attached with the manuscript.

## References

- [1] H. Bagheri, Z. Ayazi, M. Naderi, Conductive polymer-based microextraction methods: a review, *Anal. Chim. Acta* 767 (2013) 1-13.
- [2] P.M. Beaujuge, J.R. Reynolds, Color control in  $\pi$ -conjugated organic polymers for use in electrochromic devices, *Chem. Rev.* 110 (2010) 268-320.
- [3] R. Zheng, Y. Fan, Y. Wang, Z. Wan, C. Jia, X. Weng, J. Xie, L. Deng, A bifunctional triphenylamine-based electrochromic polymer with excellent self-healing performance, *Electrochim. Acta* 286 (2018) 296-303.
- [4] S. Soylemez, H.Z. Kaya, Y.A. Udum, L. Toppare, A multipurpose conjugated polymer: Electrochromic device and biosensor construction for glucose detection, *Org. Electron.* 65 (2019) 327-333.
- [5] Ş.C. Cevher, D. Keles, G. Hizalan, L. Toppare, A. Cirpan, Alkyl-end phenanthroimidazole modification of benzotriazole based conjugated polymers for optoelectronic applications, *Synthetic Met.* 244 (2018) 1-9.
- [6] J. Liu, L. Li, R. Xu, K. Zhang, M. Ouyang, W. Li, X. Lv, C. Zhang, Design, synthesis and properties of donor-acceptor-donor' asymmetric structured electrochromic polymers based on fluorenone as acceptor units, *ACS Appl. Polym. Mater.* 1 (2019) 1081-1087.
- [7] H. Yu, S. Shao, L. Yan, H. Meng, Y. He, C. Yao, P. Xu, X. Zhang, W. Hu, W. Huang, Side-chain engineering of green color electrochromic polymer materials: toward adaptive camouflage application, *J. Mater. Chem. C* 4 (2016) 2269-2273.

- [8] H. Gu, S. Ming, K. Lin, S. Chen, X. Liu, B. Lu, J. Xu, Isoindigo as an electron- deficient unit for high- performance polymeric electrochromics, *Electrochim. Acta*, 260 (2018) 772-782.
- [9] G. Ding, C.M. Cho, C. Chen, D. Zhou, X. Wang, A.Y.X. Tan, J. Xu, X. Lu, Black-to-transmissive electrochromism of azulene-based donor–acceptor copolymers complemented by poly (4-styrene sulfonic acid)-doped poly (3,4-ethylenedioxythiophene), *Org. Electron.* 14 (2013) 2748-2755.
- [10] X. Lv, W. Li, M. Ouyang, Y. Zhang, D.S. Wright, C. Zhang, Polymeric electrochromic materials with donor–acceptor structures, *J. Mater. Chem. C* 5 (2017) 12-28.
- [11] S. Mi, J. Wu, J. Liu, J. Zheng, C. Xu, Donor– $\pi$ -bridge–acceptor fluorescent polymers based on thiophene and triphenylamine derivatives as solution processable electrochromic materials, *Org. Electron.* 23 (2015) 116-123. .
- [12] H.J. Yen, C.J. Chen, G.S. Liou, Flexible multi-colored electrochromic and volatile polymer memory devices derived from starburst triarylamine-based electroactive polyimide, *Adv. Funct. Mater.* 23 (2013) 5307-5316.
- [13] J. Sun, Y. Dai, M. Ouyang, Y. Zhang, L. Zhan, C. Zhang, Unique torsional cruciform  $\pi$ -architectures composed of donor and acceptor axes exhibiting mechanochromic and electrochromic properties, *J. Mater. Chem. C*, 3 (2015) 3356-3363.
- [14] F.B. Koyuncu, An ambipolar electrochromic polymer based on carbazole and naphthalene bisimide: Synthesis and electro-optical properties, *Electrochim. Acta* 68 (2012) 184-191.
- [15] G. Hızalan, A. Balan, D. Baran, L. Toppare, Spray processable ambipolar benzotriazole bearing electrochromic polymers with multi-colored and transmissive states, *J. Mater. Chem.* 21 (2011) 1804-1809.
- [16] C. Xu, J. Zhao, M. Wang, C. Cui, R. Liu, Electrosynthesis and characterization of a donor–acceptor type electrochromic material from poly(4,7-dicarbazol-9-yl-2,1,3-benzothiadiazole) and its application in electrochromic devices, *Thin Solid Films* 527 (2013) 232-238.
- [17] S. Tarkuc, Y.A. Udum, L. Toppare, Tailoring the optoelectronic properties of donor-acceptor-donor type  $\pi$ -conjugated polymers via incorporating different electron-acceptor moieties, *Thin Solid Films* 520 (2012) 2960-2965.

- [18] T. Soganci, H.C. Soyleyici, M. Ak, A soluble and fluorescent new type thienylpyrrole based conjugated polymer: optical, electrical and electrochemical properties, *Phys. Chem. Chem. Phys.* 18 (2016) 14401-14407.
- [19] W.T. Neo, Q. Ye, X. Wang, H. Yan, J. Xu, Low band-gap polymers incorporating benzotriazole and 5, 6-dialkoxy benzothiadiazole as solution processable electrochromic materials, *Express Polym. Lett.* 9 (2015) 496-508.
- [20] S. Suganya, N. Kim, J.Y. Jeong, J.S. Park, Benzotriazole-based donor-acceptor type low band gap polymers with a siloxane-terminated side-chain for electrochromic applications, *Polymer* 116 (2017) 226-232.
- [21] A. Balan, D. Baran, G. Gunbas, A. Durmus, F. Ozyurt, L. Toppare, One polymer for all: benzotriazole containing donor-acceptor type polymer as a multi-purpose material, *Chem. Commun.* 44 (2009) 6768-6770.
- [22] A. Balan, G. Gunbas, A. Durmus, L. Toppare, Donor-acceptor polymer with benzotriazole moiety: enhancing the electrochromic properties of the "Donor Unit", *Chem. Mater.* 20 (2008) 7510-7513.
- [23] D. Baran, A. Balan, S. Celebi, B.M. Esteban, H. Neugebauer, N.S. Sariciftci, L. Toppare, Processable multipurpose conjugated polymer for electrochromic and photovoltaic applications, *Chem. Mater.* 22 (2010) 2978-2987.
- [24] J.Y. Lee, S.Y. Han, B. Lim, Y.C. Nah, A novel quinoxaline-based donor-acceptor type electrochromic polymer, *J. Ind. Eng. Chem.* 70 (2019) 380-384.
- [25] S. Chen, D. Zhang, M. Wang, L. Kong, J. Zhao, Donor-acceptor type polymers containing the 2,3-bis(2-pyridyl)-5,8-dibromoquinoxaline acceptor and different thiophene donors: electrochemical, spectroelectrochemistry and electrochromic properties, *New J. Chem.* 40 (2016) 2178-2188.
- [26] A. Durmus, G.E. Gunbas, L. Toppare, New, highly stable electrochromic polymers from 3,4-ethylenedioxythiophene-bis-substituted quinoxalines toward green polymeric materials, *Chem. Mater.* 19 (2007) 6247-6251.
- [27] G.E. Gunbas, A. Durmus, L. Toppare, Could green be greener? Novel donor-acceptor-type electrochromic polymers: towards excellent neutral green materials with exceptional

- transmissive oxidized states for completion of RGB color space, *Adv. Mater.* 20 (2008) 691-695.
- [28] G.E. Gunbas, A. Durmus, L. Toppare, A unique processable green polymer with a transmissive oxidized state for realization of potential RGB-based electrochromic device applications, *Advanced Funct. Mater.* 18 (2008) 2026-2030.
- [29] Y. Zhang, L. Kong, X. Ju, J. Zhao, Effects of fluoro substitution on the electrochromic performance of alternating benzotriazole and benzothiadiazole-based donor-acceptor type copolymers, *Polymers* 10 (2018) 23.
- [30] D. Zhang, M. Wang, X. Liu, J. Zhao, Synthesis and characterization of donor-acceptor type conducting polymers containing benzotriazole acceptor and benzodithiophene donor or s-indacenodithiophene donor, *RSC Adv.* 6 (2016) 94014-94023.
- [31] Xu, M. Wang, W. Fan, J. Zhao, H. Wang, The synthesis of new donor-acceptor polymers containing the 2,3-di(2-furyl)quinoxaline moiety: Fast-switching, low-band-gap, p-and n-dopable, neutral green-colored materials, *Electrochim. Acta* 160 (2015) 271-280.
- [32] J. Xu, Q. Ji, L. Kong, H. Du, X. Ju, J. Zhao, Soluble electrochromic polymers incorporating benzoselenadiazole and electron donor units (carbazole or fluorene): synthesis and electronic-optical properties, *Polymers* 10 (2018) 450.
- [33] D. Kitazawa, N. Watanabe, S. Yamamoto, J. Tsukamoto, Conjugated polymers based on quinoxaline for polymer solar cells, *Sol. Energ. Mat. Sol. C.* 98 (2012) 203-207.
- [34] M. İçli, M. Pamuk, F. Algi, A.M. Önal, A. Cihaner, A new soluble neutral state black electrochromic copolymer via a donor-acceptor approach, *Org. Electron.* 11 (2010) 1255-1260.
- [35] C.R. Moylan, R.D. Miller, R.J. Twieg, K.M. Betterton, V.Y. Lee, T.J. Matray, C. Nguyen, Synthesis and nonlinear optical properties of donor-acceptor substituted triaryl azole derivatives, *Chem. Mater.* 5 (1993) 1499-1508.
- [36] J.L. Banal, J. Subbiah, H. Graham, J.K. Lee, K.P. Ghiggino, W.W. Wong, Electron deficient conjugated polymers based on benzotriazole, *Polym. Chem.* 4 (2013) 1077-1083.
- [37] J.A. Kerszulis, K.E. Johnson, M. Kuepfert, D. Khoshabo, A.L. Dyer, J.R. Reynolds, Tuning the painter's palette: subtle steric effects on spectra and colour in conjugated electrochromic polymers, *J. Mater. Chem. C* 3 (2015) 3211-3218.

- [38] S. Celebi, A. Balan, B. Epik, D. Baran, L. Toppare, Donor acceptor type neutral state green polymer bearing pyrrole as the donor unit, *Org. Electron.* 10 (2009) 631-636.
- [39] W.T. Neo, Z. Shi, C.M. Cho, S.J. Chua, J. Xu, Effects of chemical composition, film thickness, and morphology on the electrochromic properties of donor-acceptor conjugated copolymers based on diketopyrrolopyrrole, *ChemPlusChem*, 80 (2015) 1298-1305.
- [40] X. Wang, Z. Zhang, H. Luo, S. Chen, S. Yu, H. Wang, X. Li, G. Yu, Y. Li, Effects of fluorination on the properties of thieno[3,2-b]thiophene-bridged donor- $\pi$ -acceptor polymer semiconductors, *Polym. Chem.* 5 (2014) 502-511.
- [41] J. Hou, M.H. Park, S. Zhang, Y. Yao, L.M. Chen, J.H. Li, Y. Yang, Bandgap and molecular energy level control of conjugated polymer photovoltaic materials based on benzo[1,2-b:4,5-b']dithiophene, *Macromolecules*, 41 (2008) 6012-6018.
- [42] N. Jian, H. Gu, S. Zhang, H. Liu, K. Qu, S. Chen, X. Liu, Y. He, G. Niu, S. Tai, J. Wang, B. Lu, J. Xu, Y. Yu, Synthesis and electrochromic performances of donor-acceptor-type polymers from chalcogenodiazolo[3,4-c]pyridine and alkyl ProDOTs, *Electrochim. Acta* 266 (2018) 263-275.
- [43] A. Berlin, G. Zotti, S. Zecchin, G. Schiavon, B. Vercelli, A. Zanelli, New low-gap polymers from 3,4-ethylenedioxythiophene-bis-substituted electron-poor thiophenes. The roles of thiophene, donor-acceptor alternation, and copolymerization in intrinsic conductivity, *Chem. Mater.* 16 (2004) 3667-3676.
- [44] W.T. Neo, L.M. Loo, J. Song, X. Wang, C.M. Cho, H.S.O. Chan, Y. Zong, J. Xu, Solution-processable blue-to-transmissive electrochromic benzotriazole-containing conjugated polymers, *Polym. Chem.* 4 (2013) 4663-4675.
- [45] G.E. Gunbas, P. Camurlu, I.M. Akhmedov, C. Tanyeli, A.M. Önal, L. Toppare, A fast switching, low band gap, p-and n-dopable, donor-acceptor type polymer, *J. Electroanal. Chem.* 615 (2008) 75-83.
- [46] J. Cai, H. Niu, P. Zhao, Y. Ji, L. Ma, C. Wang, X. Bai, W. Wang, Multicolored near-infrared electrochromic polyimides: Synthesis, electrochemical, and electrochromic properties, *Dyes Pigments* 99 (2013) 1124-1131.

- [47] B. Hu, W. Luo, L. Jin, Z. Liu, M. Wang, L. Zhou, C. Li, Electrochemical and spectroelectrochemical properties of poly(carbazole-EDOT)s derivatives functionalized with benzonitrile and phthalonitrile units, *ECS J. Solid State Sci. Technol.* 5 (2016) P21-P26.
- [48] W. Li, J. Ning, Y. Yin, X. Xing, M. Qi, T. Li, J. Cao, Y. He, I.F. Perepichka, H. Meng, Thieno[3,2-b]thiophene-based conjugated copolymers for solution-processable neutral black electrochromism, *Polym. Chem.* 9 (2018) 5608-5616.
- [49] G. Öktem, A. Balan, D. Baran, L. Toppare, Donor-acceptor type random copolymers for full visible light absorption, *Chem. Commun.* 47 (2011) 3933-3935.
- [50] M. Karakus, A. Balan, D. Baran, L. Toppare, A. Cirpan, Electrochemical and optical properties of solution processable benzotriazole and benzothiadiazole containing copolymers, *Synthetic Met.* 162 (2012) 79-84.
- [51] Y. Liu, M. Wang, J. Zhao, C. Cui, J. Liu, Effects of alkyl or alkoxy side chains on the electrochromic properties of four ambipolar donor-acceptor type polymers, *RSC Adv.* 4 (2014) 52712-52726.
- [52] X. Wu, W. Zhang, Q. Wang, Y. Wang, H. Yan, W. Chen, Hydrogen bonding of graphene/polyaniline composites film for solid electrochromic devices, *Synthetic Met.* 212 (2016) 1-11.
- [53] J.H. Tsai, C.C. Chueh, M.H. Lai, C.F. Wang, W.C. Chen, B.T. Ko, C. Ting, Synthesis of new indolocarbazole-acceptor alternating conjugated copolymers and their applications to thin film transistors and photovoltaic cells, *Macromolecules* 42 (2009) 1897-1905.

## Highlights

1. Three D-A type copolymers employing benzotriazole and quinoxaline units as acceptors were synthesized.
2. The different ratio of acceptors caused diverse multichromism of the polymers.
3. The polymers showed desirable electrochromic properties with medium band gaps.



## **Declaration of Interest Statement**

**Journal:** Organic Electronics

**Manuscript ID:** ORGELE-D-19-00914

**Title:** Synthesis and characterization of soluble donor-acceptor type copolymers based on benzotriazole, quinoxaline and benzene units with multicolor electrochromism

**Authors:** Yan Zhang, Hongmei Du, Yiming Yin, Yunyun Dong, Jinsheng Zhao\*,  
Zhen Xu\*

**Declaration of Interest Statement:** We declare that we have no conflict of interest for the present manuscript.